IMPULSIVE RESPONSE OF CANTILEVER BEAMS

IMPULSIVE RESPONSE OF CANTILEVER BEAMS

by

AZFAR SAEED, B.Sc. Eng.

A Thesis

submitted to the Faculty of Graduate Studies

in Partial Fulfilment of the Requirements

for the Degree of

Master of Engineering

McMaster University

April, 1966

MASTER OF ENGINEERING (1966)   McMASTER UNIVERSITY
(Civil Engineering)   Hamilton, Ontario

TITLE: Impulsive Response of Cantilever Beams

AUTHOR: Azfar Saeed, B.Sc.Eng. (Aligarh Muslim University)

SUPERVISOR: Dr. A. C. Heidebrecht

NUMBER OF PAGES: xi, 79

SCOPE AND CONTENTS:

This thesis describes the analytical and experimental study of cantilever beams subjected to impulse at their tips. Tests were conducted on four beam specimens. These tests were carried out for the purpose of investigating the validity of the theory as presented in this thesis.

ACKNOWLEDGEMENTS

iii

CONTENTS

CONTENTS (Continued)

NOTATION

A	Area of the pulse
A_{ij}, $[A]$	Coefficients of $\{U\}$ in $\{R\}$
B_i, $\{B\}$	Constant column vector in $\{R\}$
C_{ij}	Viscous damping coefficient
C_c	Critical damping coefficient
E	Modulus of elasticity
F_1	Maximum amplitude of the pulse
$F_i(t)$, $F(x,t)$	Applied dynamic forces
I	Moment of inertia of cross-section
$I.F.$	Impulse factor
M_i	Bending moment at point i
M_i^*	yield moment at point i
R_i, $\{R\}$	Resistance to deformation
$S.G.$	Strain Gage
T_1, T_2	Partial durations of the pulse
g	Acceleration of gravity
i, j	Indices
l	Length of beam
m_i	Mass at point i
n	Number of mass-points; number of degrees-of-freedom
t	Time variable

vi

t_D	Total duration of the pulse
Δt	Time interval in numerical integration
U_i, $\{U\}$	Deflections
$\dot{U}_i$	Velocity at point i
$\ddot{U}_i$	Acceleration at point i
w	Total weight of the beam
x,y	Co-ordinate directions
Δ_i	Elastic-plastic phase indicator
Σ	Indicates Summation
Φ	Curvature
δ_{ij}	Kronecker delta; $= 1$ if $i = j$; $= 0$ if $i \neq j$
Θ, Θ_i	Slope
ϵ	Strain
λ	Distances between assumed mass-points on beam
ϕ_i	Plastic-hinge rotation
X	Variable portion of ϕ_i
σ	Stress
σ^*	Yield stress
Ψ_i	Constant or residual portion of ϕ_i
$\| \|$	Absolute value of enclosed quantity
$[\ ^T]$	Transpose matrix
$[\ ]^{-1}$	Inverse matrix
$[J],[K],[L],[M],$ $[P],[Q],[S],[T],$ $[\Theta]$	Miscellaneous matrices used in derivations

vii

$\{G\},\{H\},\{K\},\{L\},\{N\},$
$\{\Omega\},\{W\},\{Z\},\{\Gamma\}$ Miscellaneous column vectors used in derivations

All quantities with a horizontal bar over them are non-dimensional forms of the original quantities unless defined otherwise.

LIST OF FIGURES

LIST OF FIGURES (Continued)

LIST OF TABLES

CHAPTER I

Introduction

1.1 General

In this dissertation an analytical method is presented for evaluating the dynamic response of inelastic cantilever beams subjected to impulsive loads at their tips. Use was made of an I.B.M. 7040 digital computer for carrying out the analytical work which involved a single step forward numerical integration procedure. The experimental work was performed in order to check the validity of the theory.

1.2 Previous Work

Parkes[1*], in analysing a cantilever beam struck transversely at the tip, assumed a rigid plastic material. His experimental program consisted of testing cantilever beams of various lengths. These beams were struck either by weights falling through a small height (heavy strikers), or by rifle bullets (light strikers). For light strikers different yield stress values were used for different rates of strain, as given by Manjoine[2]. The average value of dynamic plastic moment used for heavy strikers was 1.5 times the static value. A good degree of agreement was found between experimental and analytical values.

---

* Numbers refer to the Bibliography listing.

Mentel[3] published analytical and experimental results for the plastic deformation of a cantilever beam with an attached tip mass. The beam was subjected to a transverse acceleration applied at its base. The analysis was based on a rigid-plastic behaviour. The experimental results showed that a correction due to strain-rate effect was necessary to the theory in order to obtain better agreement.

Similar experiments were carried out by Bodner and Symonds[4,5] on cantilever beam specimens of mild steel and aluminum alloy. These were essentially improvements on Mentel's experiments. However again it was found that the principal cause of discrepancies between theoretical and experimental results was strain rate.

Schultz[6,7] and Blanchard[8] used a lumped-mass approach for computing the response of cantilever beams subjected to ground acceleration. The computations were carried out on digital and analog computers. The ground acceleration was applied in the form of the following pulses:

1) Half - Sine

2) Rectangular

3) Triangular

The response was computed for equal area and equal amplitude pulses. The results obtained by Schultz and Blanchard agree in principle with those presented in this investigation.

1.3 Analytical Work

The elasto-plastic and elastic response of the cantilever beam subjected to a triangular pulse at the tip is studied. The analysis, based on the assumption that the material of the beam is elastic-perfectly-plastic, is described in Chapter II. Duration and area are the two important parameters of a triangular pulse. The following two combinations of these parameters are considered:

a) Area constant with changing duration.

b) Duration constant with changing area.

Curves are plotted for these results in Chapter III. Graphs showing beam shapes at maximum tip deflection are also included.

1.4 Experimental Work

The cantilever beams were struck at the tip from below by a moving mass, which fell back under gravity after striking. This was done to achieve a short contact between the beam and the striker. During the experiments recordings were made of impulsive force and the strains at various points of the beam. Permanent deflections at such points were evaluated using a theodolite.

Theoretical response was computed using the recorded impulsive force and the values obtained were compared with those measured.

CHAPTER II

Analysis

2.1 Basis of Analysis

A method describing the dynamic analysis of simply supported
and continuous beams, approximated by lumped masses, was given by
Heidebrecht, Fleming and Lee[9]. The analysis was based on a rotation
stiffness matrix and a moment matrix. These matrices, with modifications
for a cantilever beam, are the basis of the analysis presented herein.

2.2 Basic Assumptions

As is done in most analyses of this type, the stress-strain
relationship is assumed to be of an idealized form as shown in Fig.
2.1a. This requires the material of the beams to be elastic-perfectly-
plastic. Also, the moment-curvature relationship is assumed to be
idealized as shown in Fig. 2.1b. This means that the shape factor
is assumed to be unity, which is approximately true for only wide flange
and I sections.

2.3 Actual and Simplified Beam

An actual cantilever beam of length 1 and loaded with a general
dynamic loading is shown in Fig. 2.2a. The solution for the beam response
is quite complicated because of the infinite number of degree-of freedom.
In order to simplify the problem, the beam is replaced by a mathematical
model as illustrated in Fig. 2.2b. This model consists of n equal masses

- 4 -

(a) STRESS—STRAIN RELATIONSHIP

(b) MOMENT—CURVATURE RELATIONSHIP
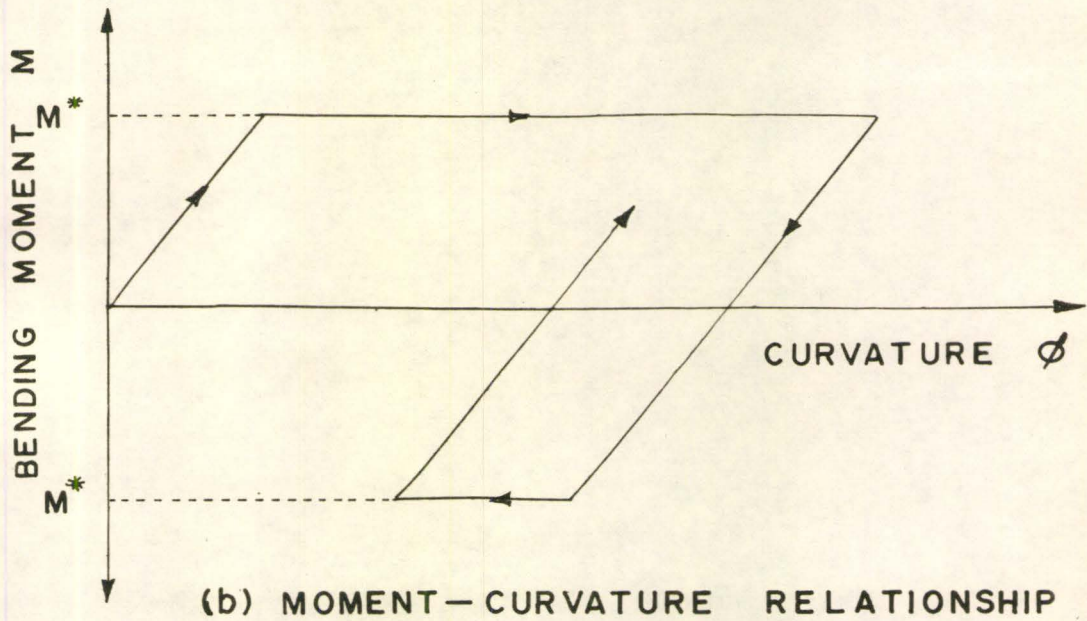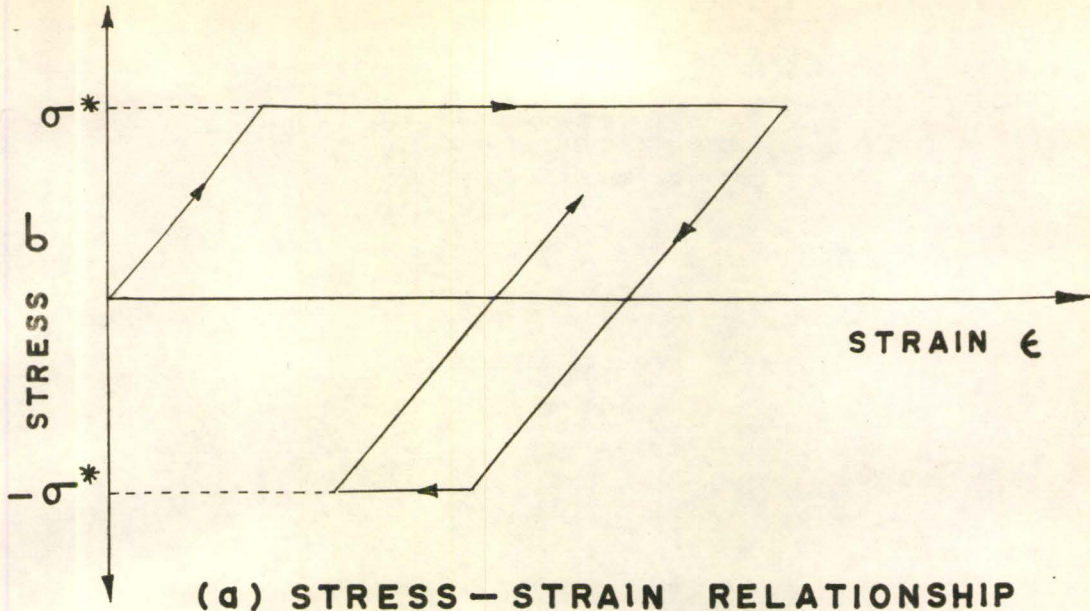
Figure 2.1   Assumptions in the Behavior of Idealized
Elastic-plastic Material
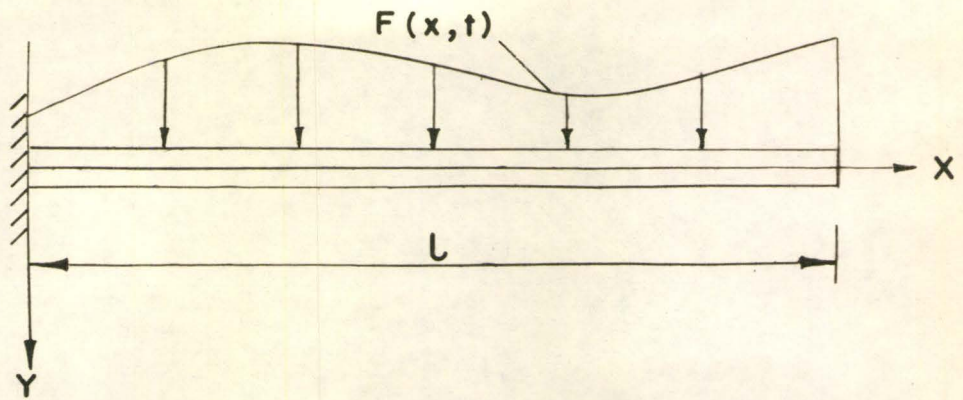
(a) ACTUAL BEAM
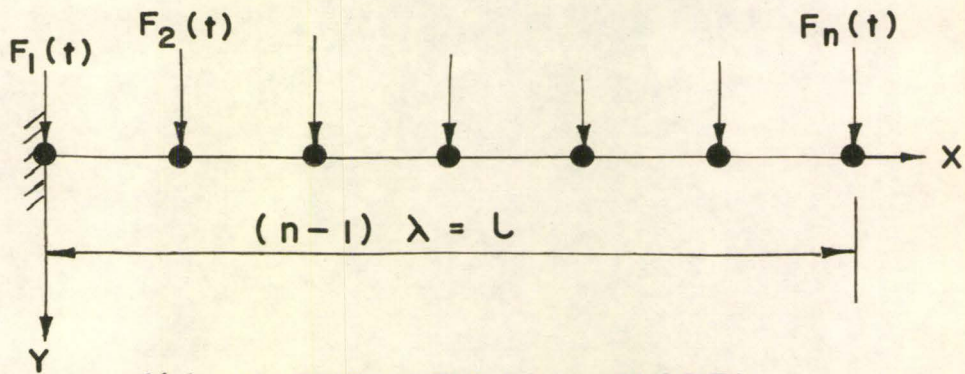
(b) MATHEMATICAL MODEL

Figure 2.2 Actual and Simplified Cantilever Beam

which are spaced at a distance λ apart. All the mass of the beam is thought of as being concentrated at these mass points. The n masses are assumed to be connected together by means of weightless elastic segments, which have the same elastic-plastic properties as the actual beam.

In Fig. 2.2b if it is assumed that w is the total weight of the beam, then for a uniform beam the mass at any point i is:

$$m_i = \frac{w}{(n-1)g} \quad (i = 1,2, \ldots\ldots\ldots n) \tag{2.1}$$

where g is acceleration due to gravity. It should be noted here that under the dynamic loading the plastic hinges can only be formed at these concentrated mass points.

2.4 Damping

In this analysis a viscous type of damping is assumed. This damping is taken to be linearly proportional to the transverse velocity at each mass point. The damping factor used is a certain percentage of the critical damping coefficient. The critical damping coefficient is assumed to be the same as that for a single mass oscillator. The critical damping coefficient C_c for a single mass oscillator is given by the equation:

$$C_c = 2\sqrt{\frac{3EI\ w}{g\ l^3}} \tag{2.2}$$

in which EI is the flexural rigidity of the beam.

2.5 Rotation and Moment Matrices

A cantilever beam model in its deflected form is shown in Fig. 2.3a. In this figure R_i is the resisting force at the mass point i. The preliminary requirement for solving such a beam under dynamic loading is the same as given in reference (9). This is to say that the resisting forces should be expressed in terms of the deformed beam shape at all times. The beam can either be in the elastic or in one of several elastic-plastic modes, depending on the number of plastic hinges existing. A relationship should also be established between the deflections, bending moments and plastic hinge rotations at each mass-point.

Fig. 2.3b shows the bending moment diagram for the beam in Fig. 2.3a. Let M_i, M_i* and ϕ_i be the bending moment, positive yield moment and the plastic hinge rotation respectively at any mass point i. At any mass point i which is elastic M_i is a variable quantity and $\phi_i = 0$ or some other constant. At any mass point j where a plastic hinge exists, $|M_j| = M_j$* and ϕ_j is a variable quantity, where $|M_j|$ denotes the absolute value of M_j.

The conjugate beam method given by Lee[10] is also used in this analysis in the same manner as it was used by Heidebrecht[9] et al. Fig. 2.3c shows the conjugate of the cantilever beam of Fig. 2.3a. Fig. 2.4 shows a segment of the beam between two consecutive masses m_i and m_{i+1}.
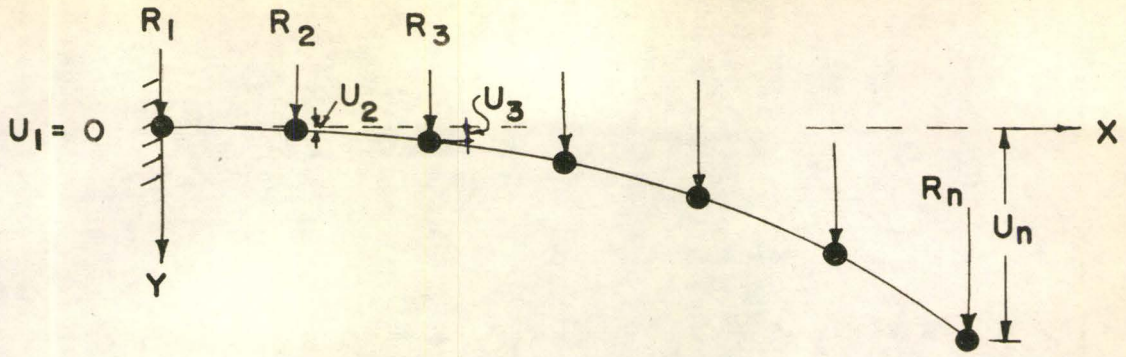
(a) DEFORMED BEAM MODEL
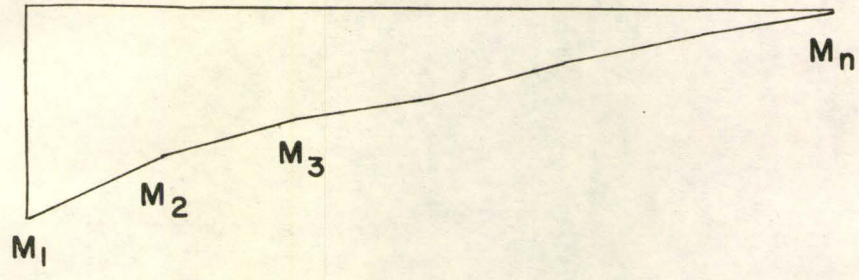
(b) BENDING MOMENT DIAGRAM
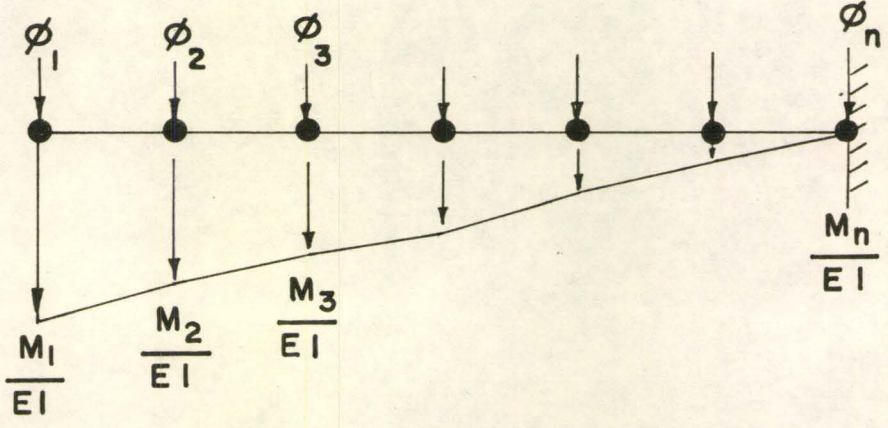
(c) CONJUGATE BEAM

Figure 2.3 Conjugate Beam Analysis
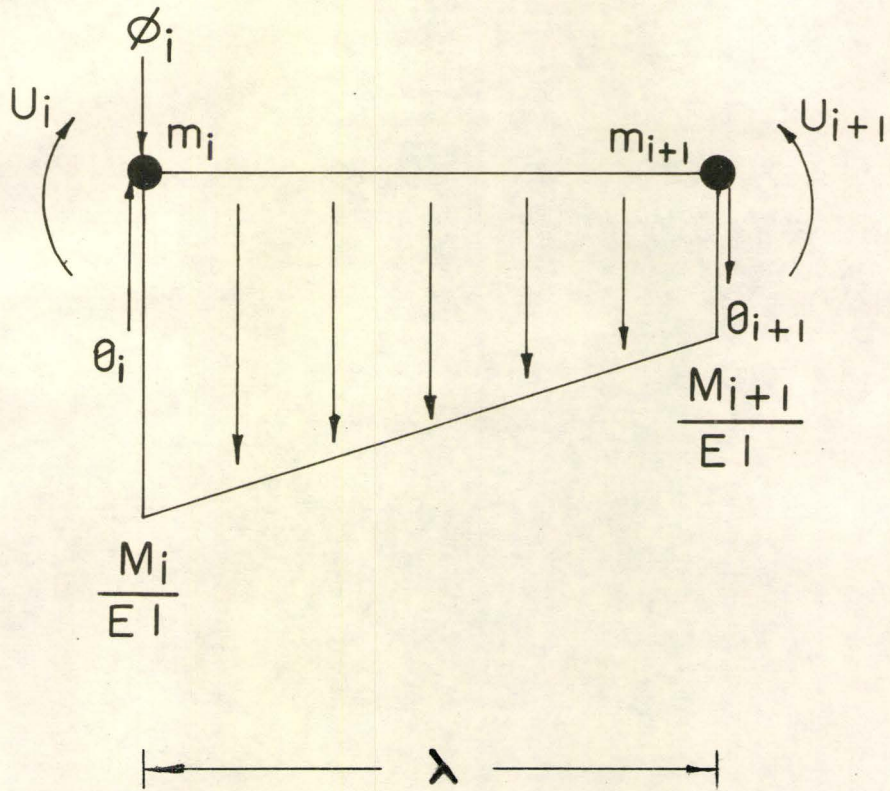
Figure 2.4 Typical Conjugate Beam Segment

The equilibrium of the segment is governed by the following recursive relationships:

$$U_{i+1} = U_i + \lambda (\theta_i - \phi_i) - \frac{\lambda^2}{6EI} (2M_i + M_{i+1}) \tag{2.3}$$

$$\theta_{i+1} = \theta_i - \phi_i - \frac{\lambda}{2EI} (M_i + M_{i+1}) \tag{2.4}$$

where U_i is the vertical deflection of mass-point i, θ_i denotes the slope of the beam immediately to the left of the mass point i.

A careful study of Eqs. 2.3 and 2.4 reveals that the deflections and slopes at all mass-points can respectively be expressed by the following matrix equations:

$$\{U\} = [P] \{\phi\} + [Q] \{M\} \tag{2.5}$$

$$\{\theta\} = [J] \{\phi\} + [K] \{M\} \tag{2.6}$$

where [P], [Q], [J] and [K] are square matrices having constant elements, {M} and {ϕ} the moment and rotation vectors respectively.

Starting from mass-point 1, the boundary conditions are:

$$U_1 = 0 \tag{2.7}$$

$$\theta_1 = \phi_1 \tag{2.8}$$

To satisfy Eq. 2.7 all elements P_{1j} and Q_{1j} (j = 1, ...n) in Eq. 2.5 should be zero. Similarly to satisfy Eq. 2.8 $J_{11} = 1$, while all the remaining elements J_{1j} (j = 2, ...n) and K_{1j} (j = 1, ...n) in Eq. 2.6 should be zero.

The following recursive relationships are derived from Eqs. 2.3 and 2.4 to find the remaining elements P_{ij} and Q_{ij} of [P] and [Q] matrices

respectively.

$$P_{(i+1)j} = P_{ij} + \lambda J_{ij} - \lambda \delta_{ij} \qquad (2.9)$$

$$Q_{(i+1)j} = Q_{ij} + \lambda K_{ij} - \frac{\lambda^2}{6EI} (2 \delta_{ij} + \delta_{(i+1)j}) \qquad (2.10)$$

where δ_{ij} is Kronecker delta which is defined as:

$$\delta_{ij} = 1 \quad \text{if } i = j$$
$$\delta_{ij} = 0 \quad \text{is } i \neq j$$

J_{ij} and K_{ij} are the elements of [J] and [K] matrices respectively.

Another recursive relationship derived from Eq. 2.4 to calculate the elements of [J] and [K] matrices is:

$$J_{(i+1)j} = J_{ij} - \delta_{ij} \qquad (2.11)$$

$$K_{(i+1)j} = K_{ij} - \frac{\lambda}{2EI} (\delta_{ij} + \delta_{(i+1)j}) \qquad (2.12)$$

[P] and [Q] matrices for a cantilever beam can be computed by using Eqs. 2.9, 2.10, 2.11 and 2.12 in succession.

2.6 Resistance Matrices

The equilibrium analysis of the original cantilever beam of Fig. 2.3a yields the following relationship between moment and resistance matrices:

$$\{M\} = \lambda [P^T] \{R\} \qquad (2.13)$$

in which $\{R\}$ is the resistance matrix and $[P^T]$ is the transpose of the matrix [P].

The remaining derivation of the resistance matrix is exactly the same as in reference (9) and is given in Appendix. The final non-dimensional form of the resistance matrix is:

$$\{\overline{R}\} = [\overline{A}] \{\overline{U}\} + \{\overline{B}\} \tag{2.14}$$

in which $\{\overline{U}\}$ is the nondimensional deflection vector and

$$[\overline{A}] = [\overline{P}^T]^{-1} [\overline{T}] \tag{2.15}$$

$$\{\overline{B}\} = [\overline{P}^T]^{-1} \{\overline{L}\} \tag{2.16}$$

where $[\overline{P}^T]^{-1}$ is the inverse of the nondimensional form of $[P^T]$, $[\overline{T}]$ and $\{\overline{L}\}$ are as defined in reference (9) and Appendix.

In dimensional form Eq. (2.14) may be written as:

$$\{R\} = [A] \{U\} + \{B\} \tag{2.17}$$

in which

$$[A] = \frac{\lambda^3}{EI} [\overline{A}] \tag{2.18}$$

and

$$\{B\} = \frac{\lambda^2}{EI} \{\overline{B}\} \tag{2.19}$$

The elements of the matrices [A] and {B} remain constant during any phase of deformation.

Proceeding in accordance with reference (9), the bending moment and plastic hinge rotation matrices are as follows:

$$\{M\} = \frac{EI}{\lambda^2} [\overline{T}] \{\overline{U}\} + \frac{EI}{\lambda} \{\overline{L}\} \tag{2.20}$$

$$\{\phi\} = \frac{1}{\lambda} [\overline{\Theta}] \{\overline{U}\} + \{K\} \tag{2.21}$$

in which $[\overline{\Theta}]$ and $\{K\}$ are as defined in Appendix.

The resisting function given by Eq. 2.17 is in a form that can directly be substituted in the differential equations of motion, which are described in section 2.7. Eqs. 2.20 and 2.21 express bending moments and plastic hinge rotation in terms of deflections for any elastic-plastic phase of the beam.

2.7 Differential Equation of Motion

The general form of the equation of motion for a multi-degree of freedom system with viscous damping as shown by Heidebrecht[11] is:

$$F_i(t) - R_i - \sum_{j=1}^{n} C_{ij} \dot{U}_j = m_i \ddot{U}_i \quad (i=1,2, \ldots n) \tag{2.22}$$

where $F_i(t)$ is the dynamic force applied, C_{ij} is the viscous damping coefficient. The velocity and acceleration are respectively denoted by $\dot{U}_i$ and $\ddot{U}_i$.

Eq. 2.16 can be written in the form:

$$R_i = \sum_{j=1}^{n} A_{ij} U_j + B_i \quad (i=1,2,\ldots n) \tag{2.23}$$

in which A_{ij} and B_i are respectively the elements of [A] and {B} matrices.

Substituting the value of R_i from Eq. 2.23 in Eq. 2.22 yields

$$F_i(t) - \sum_{j=1}^{n} A_{ij} U_j - B_i - \sum_{j=1}^{n} C_{ij} \dot{U}_j = m_i \ddot{U}_i \tag{2.24}$$

2.8 Numerical Integration Procedure

It is convenient to solve Eq. 2.24 by a single step forward integration procedure developed by Fleming and Romualdi[12]. This method assumes the deflection-velocity and velocity-acceleration relationships

to be linear over a short interval of time. These relations may be written as:

$$\ddot{U}_i(t_2) = \frac{2}{\Delta t} \ [\dot{U}_i(t_2) - \dot{U}_i(t_1)] - \ddot{U}_i(t_1) \tag{2.25}$$

$$\dot{U}_i(t_2) = \frac{2}{\Delta t} \ [U_i(t_2) - U_i(t_1)] - \dot{U}_i(t_1) \tag{2.26}$$

in which $\Delta t = t_2 - t_1$, and t is the time variable.

Substitution of Eq. 2.26 in Eq. 2.25 gives:

$$\ddot{U}_i(t_2) = \frac{4}{(\Delta t)^2} [U_i(t_2) - U_i(t_1)] - \frac{4}{\Delta t} \dot{U}_i(t_1) - \ddot{U}_i(t_1) \tag{2.27}$$

Substituting the values of $\dot{U}_i(t_2)$ and $\ddot{U}_i(t_2)$ from Eqs. 2.26 and 2.27 into Eq. 2.24 yields:

$$\sum_{j=1}^{n} K_{ij} U_j(t_2) = \sum_{j=1}^{n} L_{ij} U_j(t_1) + \sum_{j=1}^{n} M_{ij} \dot{U}_j(t_1) + \dot{m}_i \dot{U}_i(t_1) + N_i \tag{2.28}$$

in which

$$K_{ij} = \frac{4}{(\Delta t)^2} \ \delta_{ij} m_i + \frac{2}{\Delta t} C_{ij} + A_{ij}$$

$$L_{ij} = \frac{4}{(\Delta t)^2} \ \delta_{ij} m_i + \frac{2}{\Delta t} C_{ij}$$

$$M_{ij} = \frac{4}{\Delta t} \ \delta_{ij} m_i + C_{ij}$$

$$N_i = F_i(t_2) - B_i$$

The general form of the equation of motion used to find the numerical solution is expressed by Eq. 2.28.

In matrix form Eq. 2.28 can be written as:

$$[K] \ \{U(t_2)\} = \{\Omega\} \tag{2.29}$$

in which [K] is the square matrix whose elements are K_{ij} in Eq. 2.28 and $\{\Omega\}$ is a vector representing the right hand side of Eq. 2.28. Vector $\{\Omega\}$

consists only of the deflections and velocities at time t_1 which are known, the known applied force $F_i(t_2)$, and coefficient B_i. Thus Eq. 2.29 can be solved for deflections at time t_2 by inversion of matrix [K]. Once the deflection at time t_2 is known, velocity and acceleration can be computed by Eqs. 2.26 and 2.25 respectively. This single step forward integration procedure is repeated for further time steps.

2.9 Computer Program Outline

Input data consists of the properties of the beam, characteristics of the applied force and of the numerical integration procedure used. The matrices [P], [Q], [A] and {B} are then calculated. These are used to evaluate the matrices [K] and {Ω} of Eq. 2.29. Deflections at the end of the time interval are known from Eq. 2.29, which are utilized to determine velocities and acceleration for that time interval. The final step is to compute the bending moment and plastic hinge rotation using Eqs. 2.20 and 2.21.

For purely elastic response the above procedure is repeated until the response is known for a desired duration. For elastic-plastic response the procedure is a little different. Each time a mass point goes from elastic to plastic or from plastic to elastic, a new set of [A] and {B} matrices is calculated. The check for the elastic-plastic transition is that the moment at any mass point exceeds or equals the plastic moment. Plastic-elastic transition is checked by the plastic hinge rotation, which

becomes constant or decreases when a plastic-elastic transition occurs.

These transitions are described in detail by Heidebrecht[11], who has also given flow charts of the computer program concerning the transitions.

The rest of the structural properties are calculated in the same way as described for the elastic response.

CHAPTER III

Analytical Results

3.1 General

The analysis described in the last chapter is used to compute the elastic and elastic-plastic response of mild steel cantilever beams. The results are presented in tabular and graphical forms.

3.2 Forcing Function

The dynamic force applied to the tip of the beam is in the form of a triangular pulse. It was decided to use a triangular shape as this form closely approximates the experimental record of the impulse as shown in Fig. 5.2. However, the typical pulse shape used is a symmetrical triangle as shown in Fig. 3.1.

The response studies made may be divided into the following two classes.

   1) Area of the pulse constant with changing duration.

   2) Duration of the pulse constant with changing area.

In order to represent some of the pulse characteristics, a factor named Impulse Factor (I.F.) is introduced, which is defined as:

$$I.F. = \frac{F_1^2}{A} \quad lb./sec. \tag{3.1}$$

$$\text{AREA } A = \frac{1}{2}(F_1 / t)$$
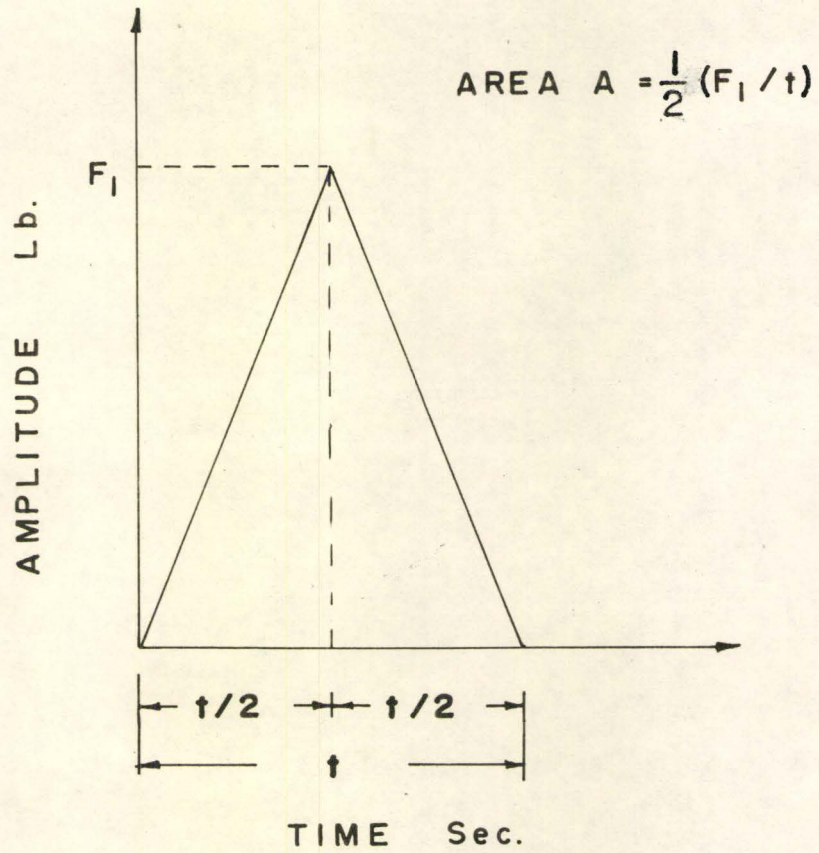
Figure 3.1 Typical Pulse Shape Applied to Series A
and B Beams

where F_1 is the maximum amplitude of the pulse in lbs., and A is the area of the pulse in lb.-sec.

Eq. 3.1 may also be written as:

$$I.F. = \frac{2F_1}{t_D} \tag{3.2}$$

where t_D is the total duration of the pulse. For a symmetrical triangular pulse Eq. 3.2 represents the slope.

3.3 Number of Degrees of Freedom

The computer program prepared can handle a system with a maximum of ten degree-of-freedom, though it can easily be modified for systems with more degrees-of-freedom. However, in order to obtain qualitatively satisfactory results and also to conserve computer time, it was decided to approximate the beams by four or five masses.

3.4 Examples

1) Series A

A typical beam analysed is shown in Fig. 3.2, and had the following characteristics:

    Length   27"

    Cross-section   1/2" x 1/2"

    Total weight   1.912 lbs.

    Yield moment (50% yield level) 47.0 ft. lb.

    Modulus of elasticity 30 x 10^6 p.s.i.
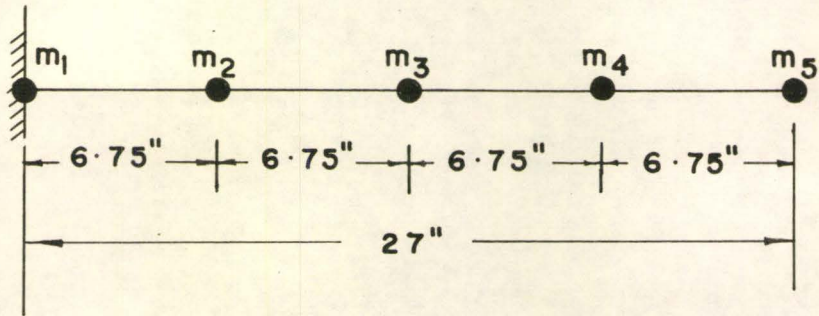
Cross − section	1/2" x 1/2"
Total weight	1·912 lbs.
Modulus of Elasticity	30×10^6 p.s.i.
Static yield moment	47·0 ft. lb.
Damping factor as percentage of critical damping coeff.	20·0

Figure 3.2   Typical Beam of Series A

Damping factor as percentage   20.0
of critical damping coefficient

Approximated by 5 masses

The forcing function used was a symmetrical triangular pulse as presented in Fig. 3.1.

Case 1: Constant Pulse Area

Table 3.1 shows the results of the elastic-plastic and elastic response for constant pulse area with changing duration. The graphical representation of elastic-plastic and elastic responses versus time is shown in Figs. 3.3 and 3.4. A comparitive representation of elastic-plastic and purely elastic responses for beam A3 is also given in Fig. 3.5. Beam shapes corresponding to Figs. 3.3 and 3.4 are shown in Figs. 3.6 and 3.7. Figs. 3.8 and 3.9 are the plots of impulse factor versus maximum tip deflection for the elastic-plastic and elastic responses respectively.

Case 2: Constant Pulse Duration

The elastic-plastic and elastic responses of beams for constant pulse duration and changing area are given in Table 3.2.

The results are graphically presented in Figs. 3.10 to 3.14.

Discussion of Series A

A study of the results indicates that for the equal area pulse, the maximum tip deflection increases as the pulse duration decreases.

Beam No.	Pulse Area	Pulse Duration	Maximum Elastic-plastic Tip Deflection	Maximum Elastic Tip Deflection	Permanent Tip Deflection Corresponding to Column 4	Plastic Hinge Rotation at Root Corresponding to Column 4	Impulse Factor x 10^{-4}
	lb.sec.	sec.	in.	in.	in.	radians	lb./sec.
1	2	3	4	5	6	7	8
A1	1.5	0.01	5.18	3.81	4.38	0.075	6.0
A2	1.5	0.02	4.48	3.47	3.74	0.075	1.5
A3	1.5	0.04	3.55	2.63	2.84	0.098	0.375
A4	1.5	0.06	2.78	1.97	1.96	0.073	0.167
A5	1.5	0.1	1.45	1.13	0.61	0.023	0.06
A6	1.5	0.2	0.62	0.62	0.00	0.00	0.015

Table 3.1: Elastic-plastic and Elastic Response of Beams for Constant Pulse Area - Series A, Case 1

Figure 3.3 Elastic-plastic Response for Equal Pulse Area - Series A
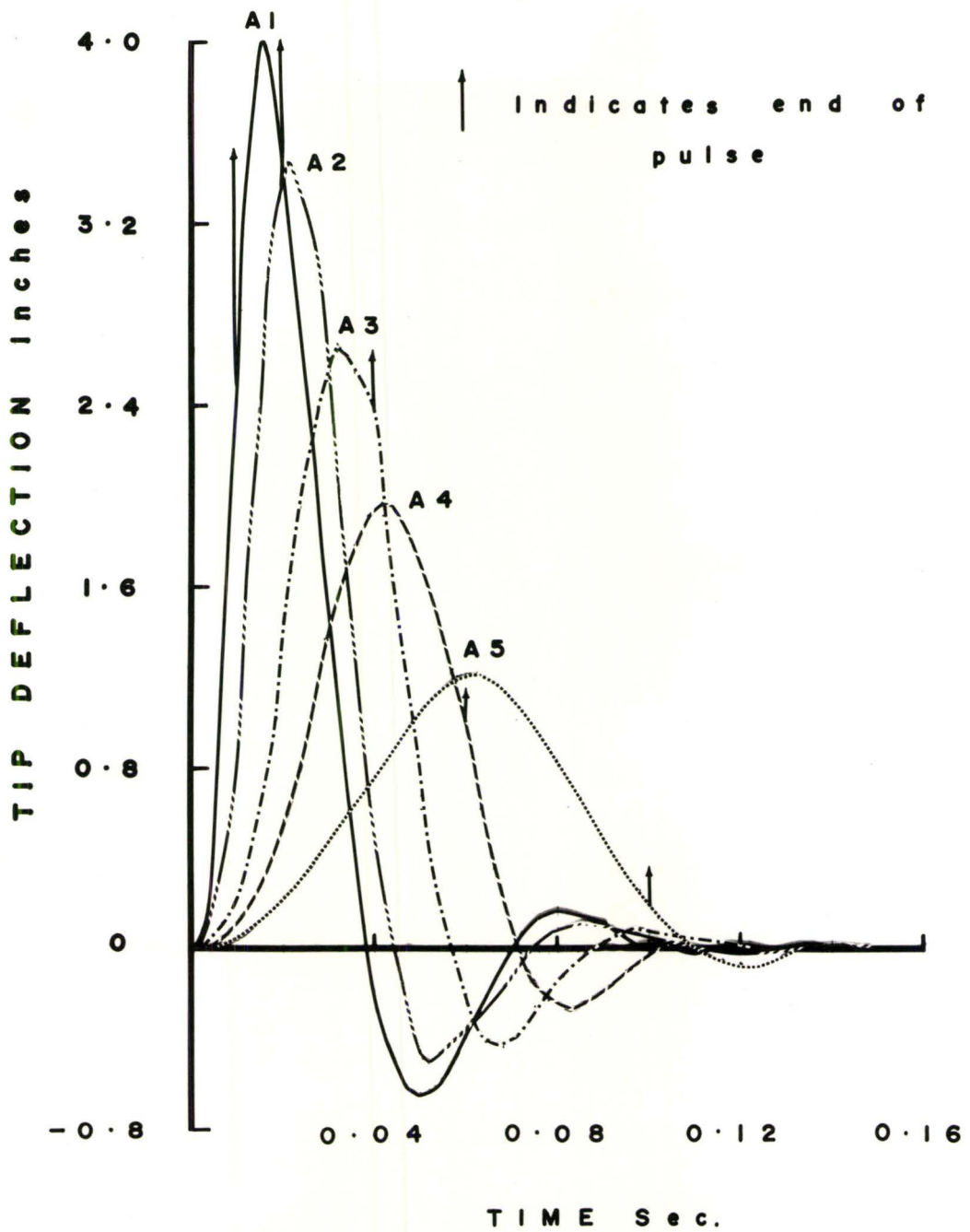
Figure 3.4 Elastic Response for Equal Pulse Area – Series A
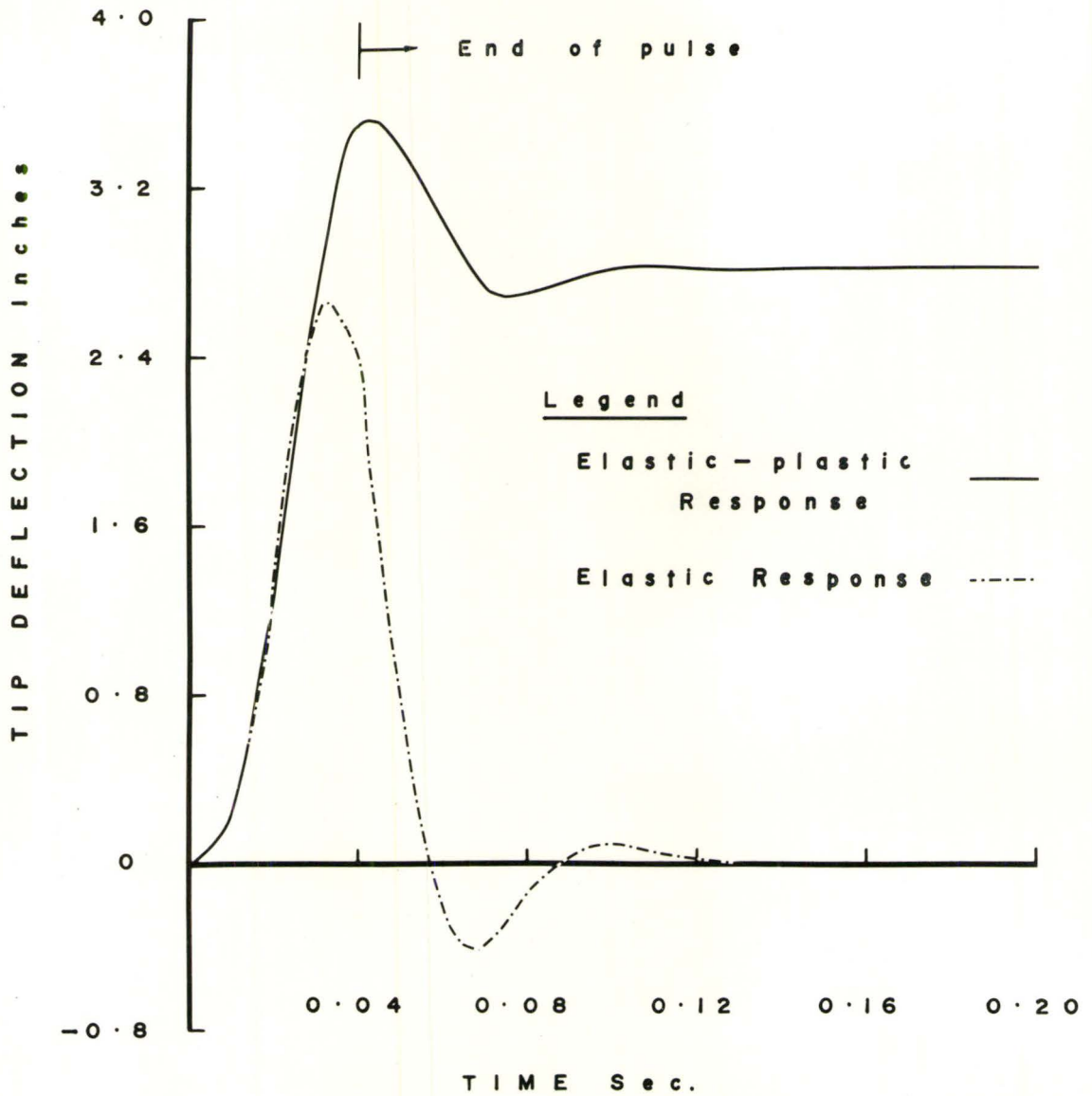
Figure 3.5 Elastic-plastic and Elastic Response of Beam A3
for Equal Pulse Area - Series A

Figure 3.6 Elastic-plastic Beam Shapes at Maximum Tip Deflection for Equal Pulse Area - Series A

Figure 3.7 Elastic Beam Shapes at Maximum Tip Deflection for Equal Pulse Area - Series A

28

Figure 3.8   Impulse Factor versus Maximum Elastic-plastic Tip Deflection for Equal Pulse Area – Series A

Figure 3.9 Impulse Factor versus Maximum Elastic Tip Deflection for Equal Pulse Area - Series A

Beam No.	Pulse Duration	Pulse Area	Maximum Elastic-plastic Tip Deflection	Maximum Elastic Tip Deflection	Permanent Tip Deflection Corresponding to Column 4	Plastic Hinge Rotation at Root Corresponding to Column 4	Impulse Factor x 10^{-4}
	sec.	lb.sec.	in.	in.	in.	radians	lb./sec.
1	2	3	4	5	6	7	8
A7	0.04	3.0	9.43	5.2	8.65	0.113	0.75
A8	0.04	1.5	3.55	2.63	2.84	0.098	0.375
A9	0.04	0.75	1.38	1.31	0.59	0.022	0.188

Table 3.2: Elastic-plastic and Elastic Response of Beams for Constant Pulse Duration - Series A,Case 2
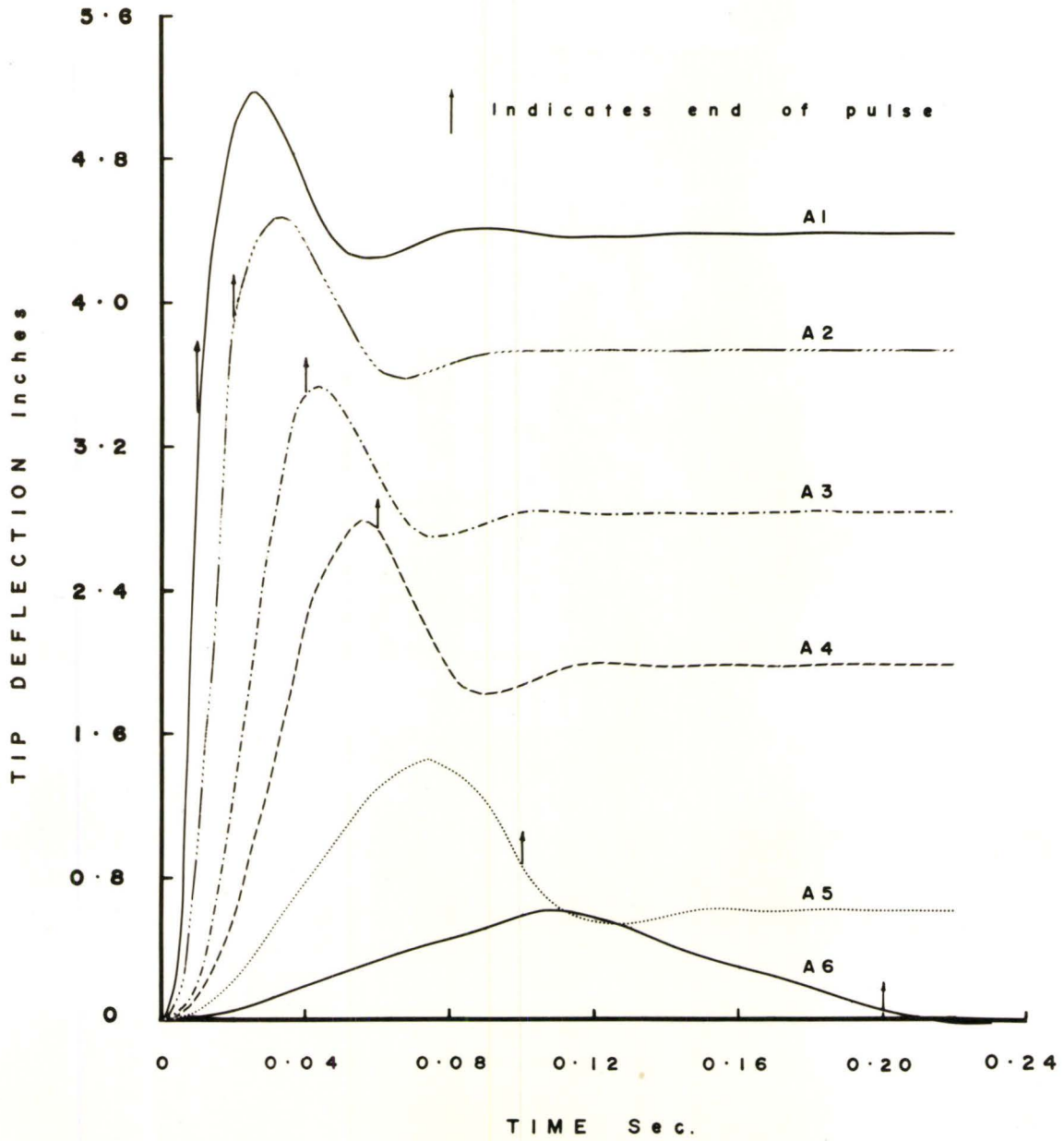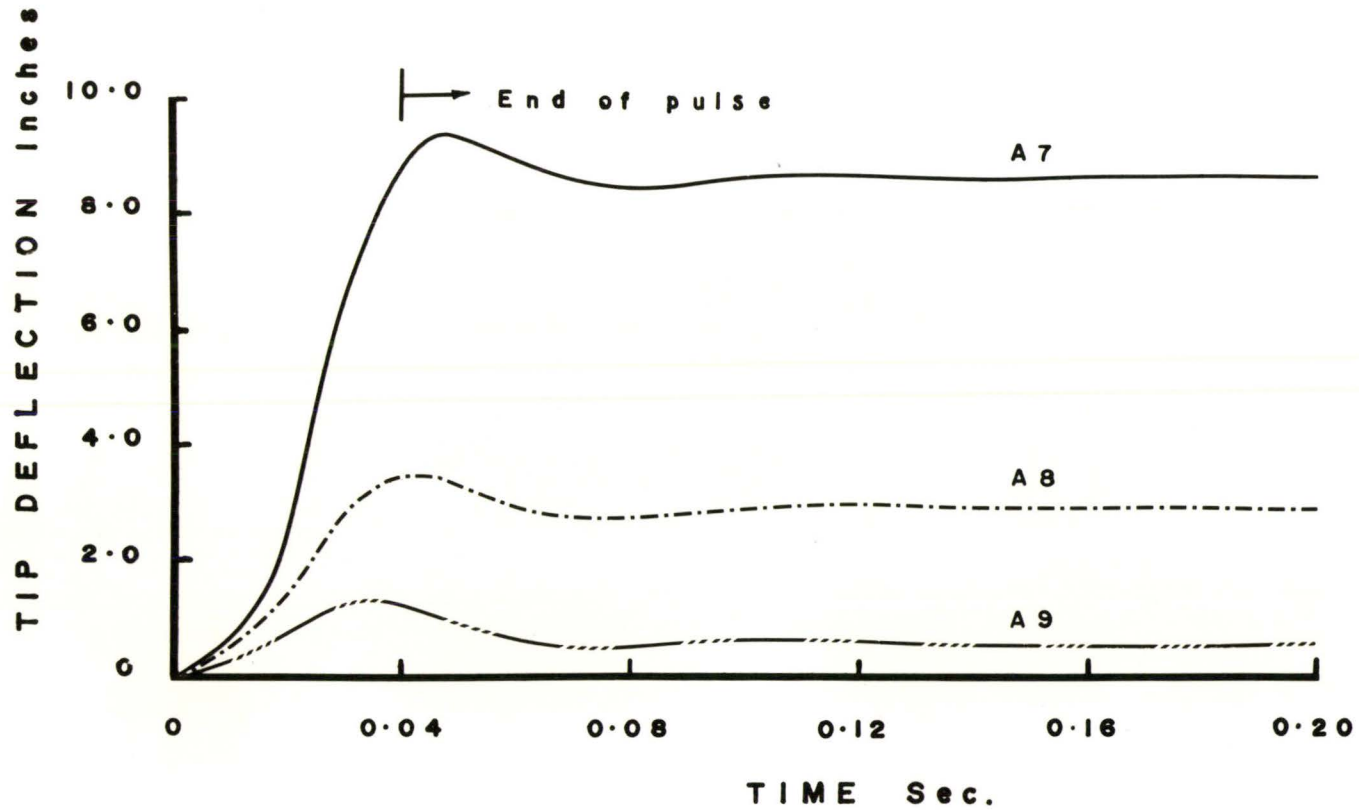
Figure 3.10 Elastic-plastic Response for Equal Pulse Duration - Series A
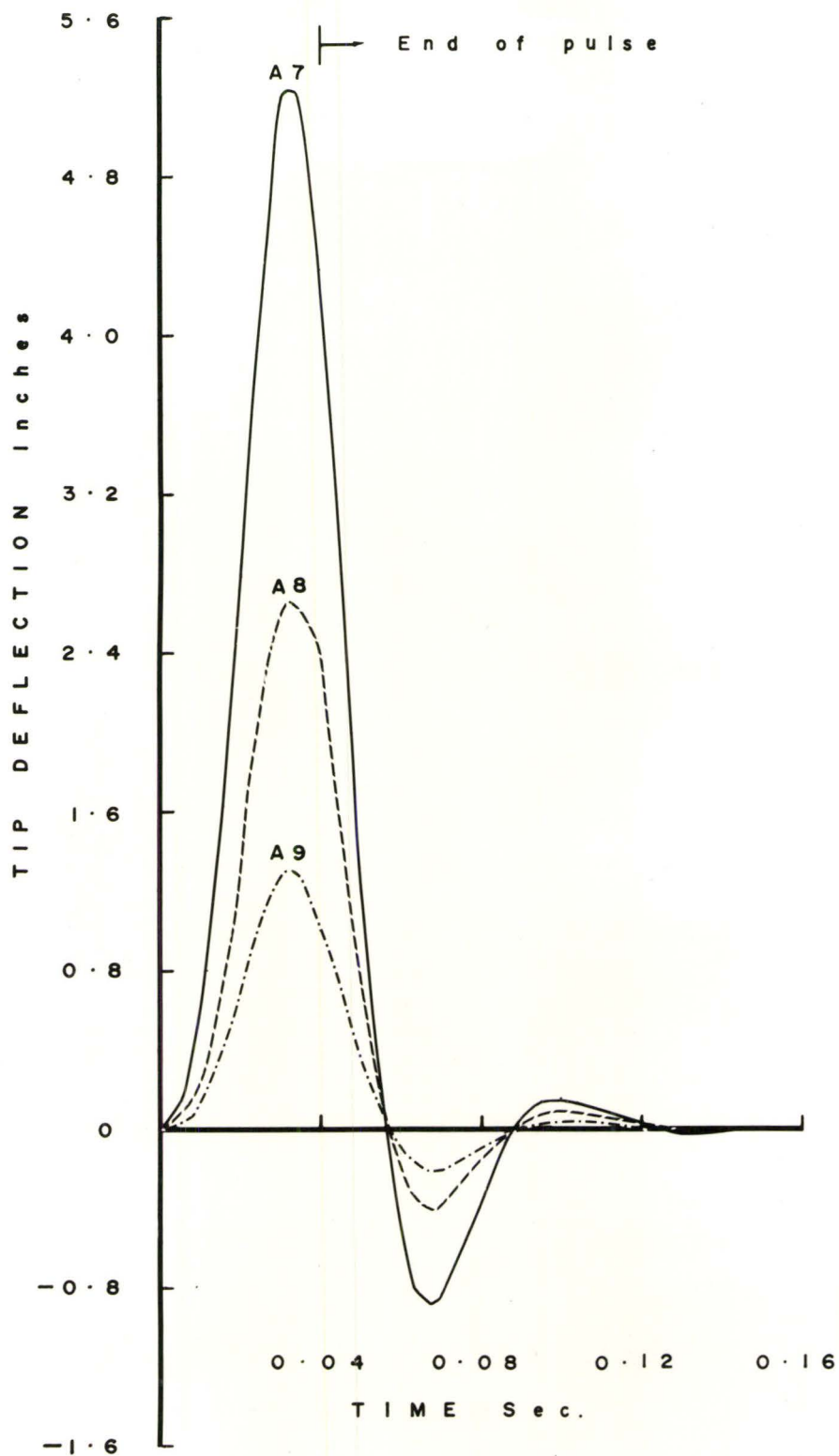
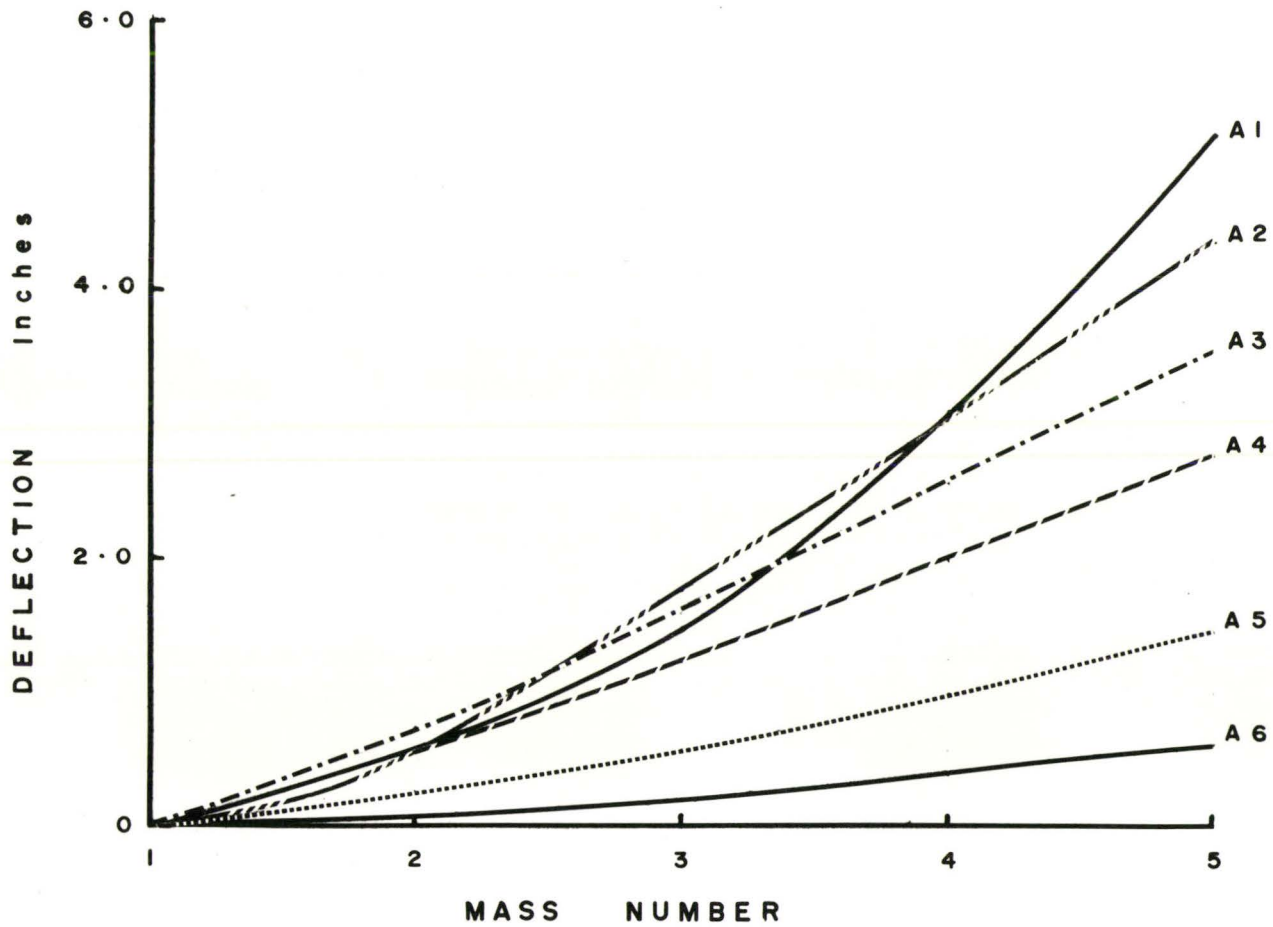Figure 3.11   Elastic Response for Equal Pulse Duration - Series A
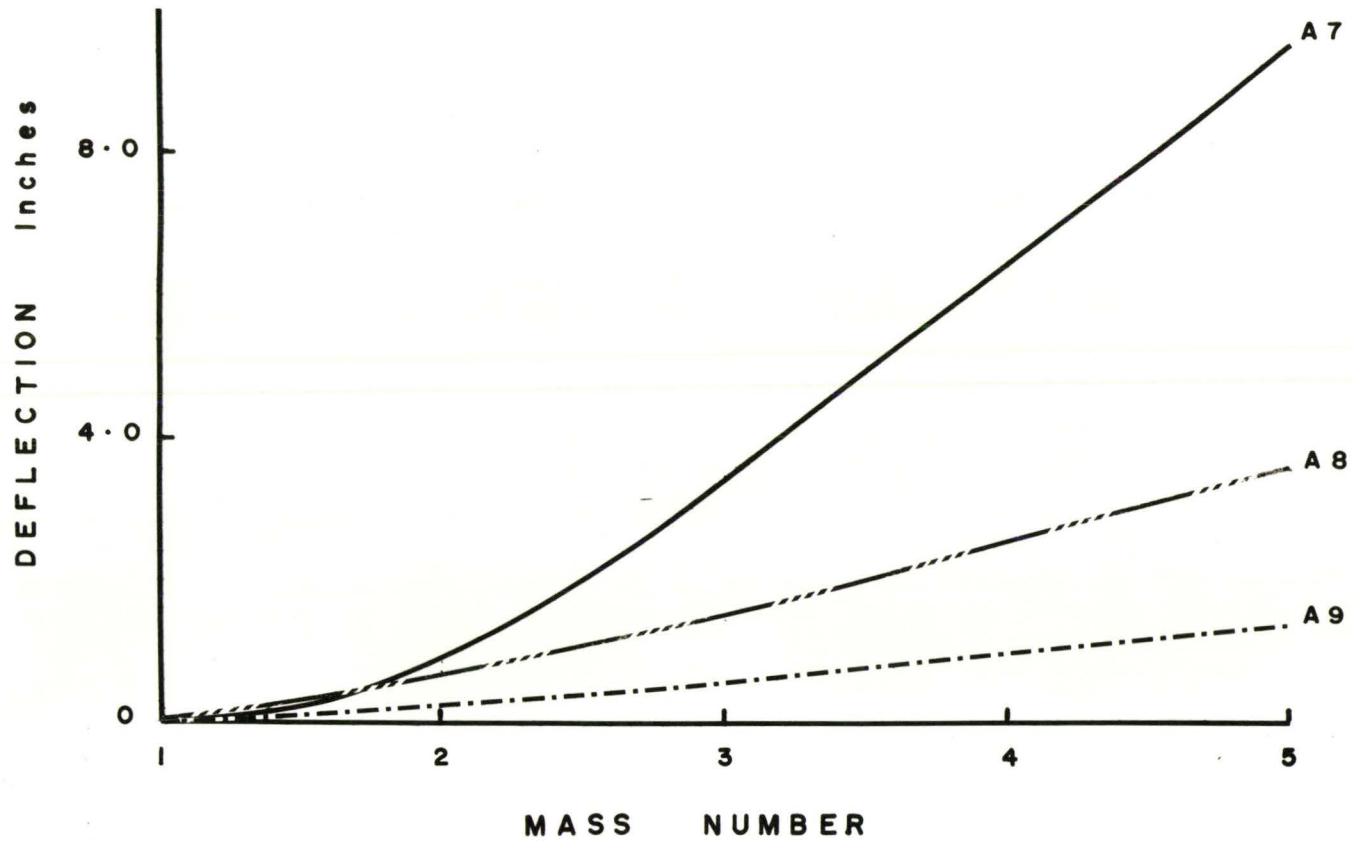
Figure 3.12   Elastic-plastic Beam Shapes at Maximum Tip Deflection for Equal Pulse Duration – Series A
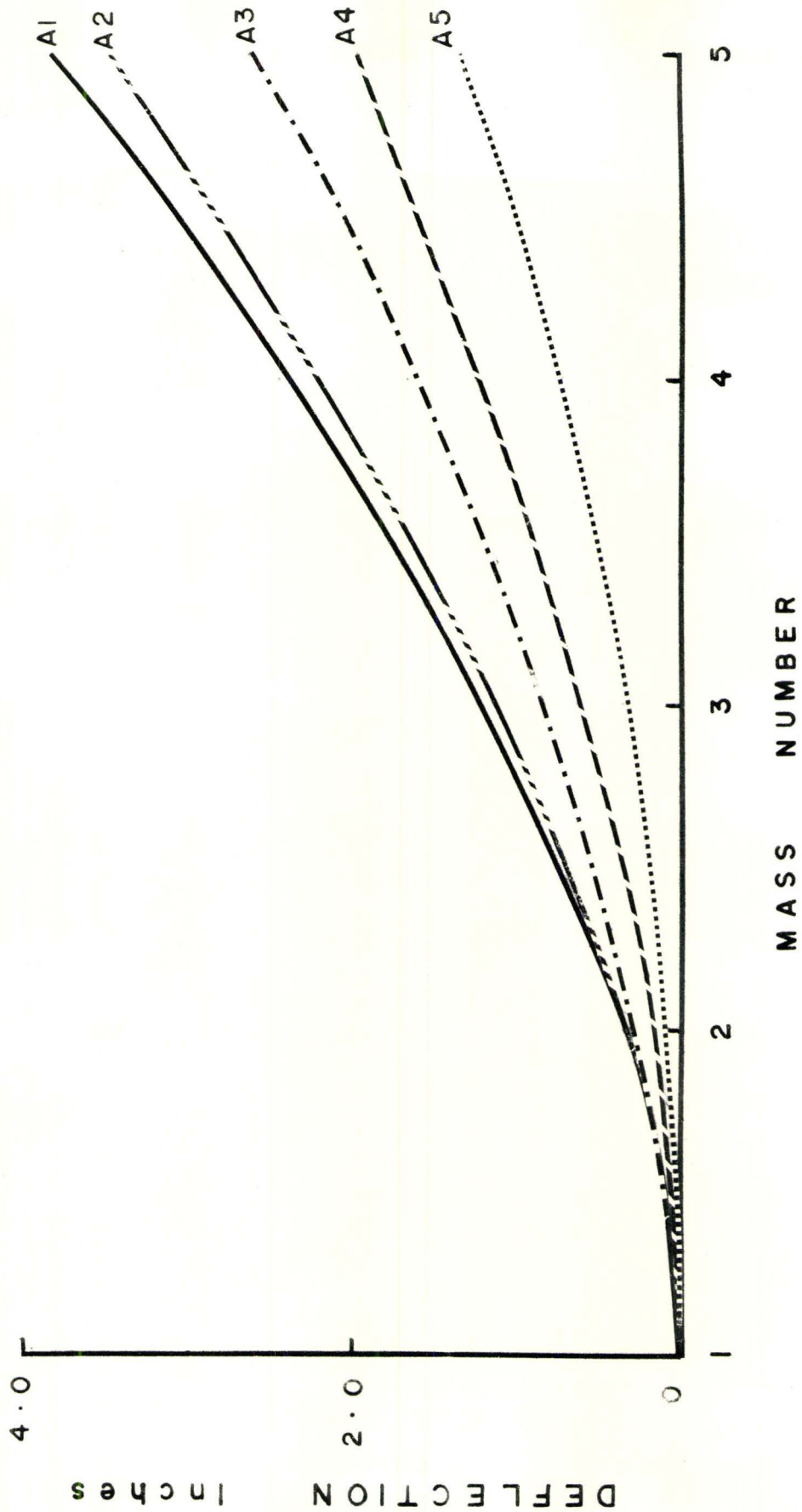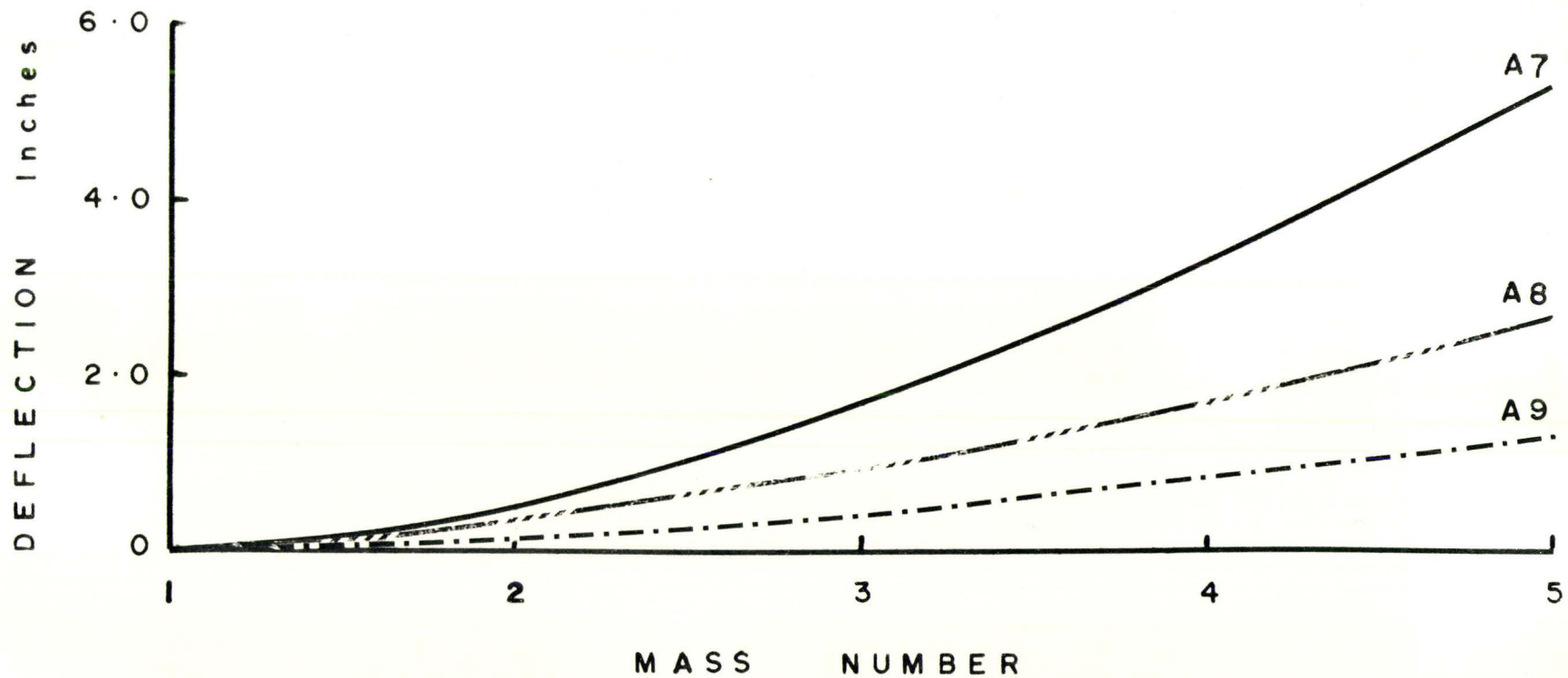
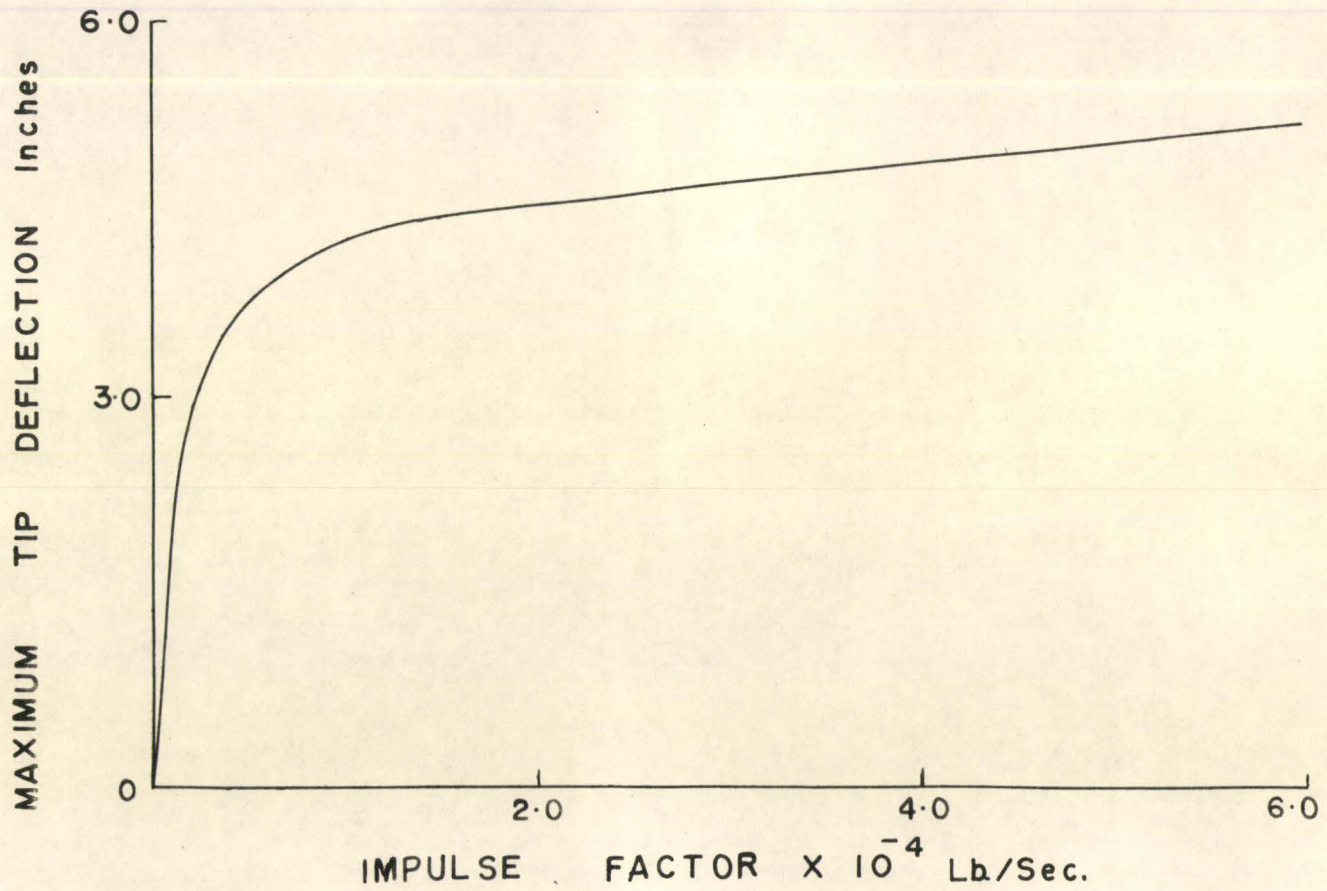Figure 3.13 Elastic Beam Shapes at Maximum Tip Deflection for Equal Pulse Duration – Series A
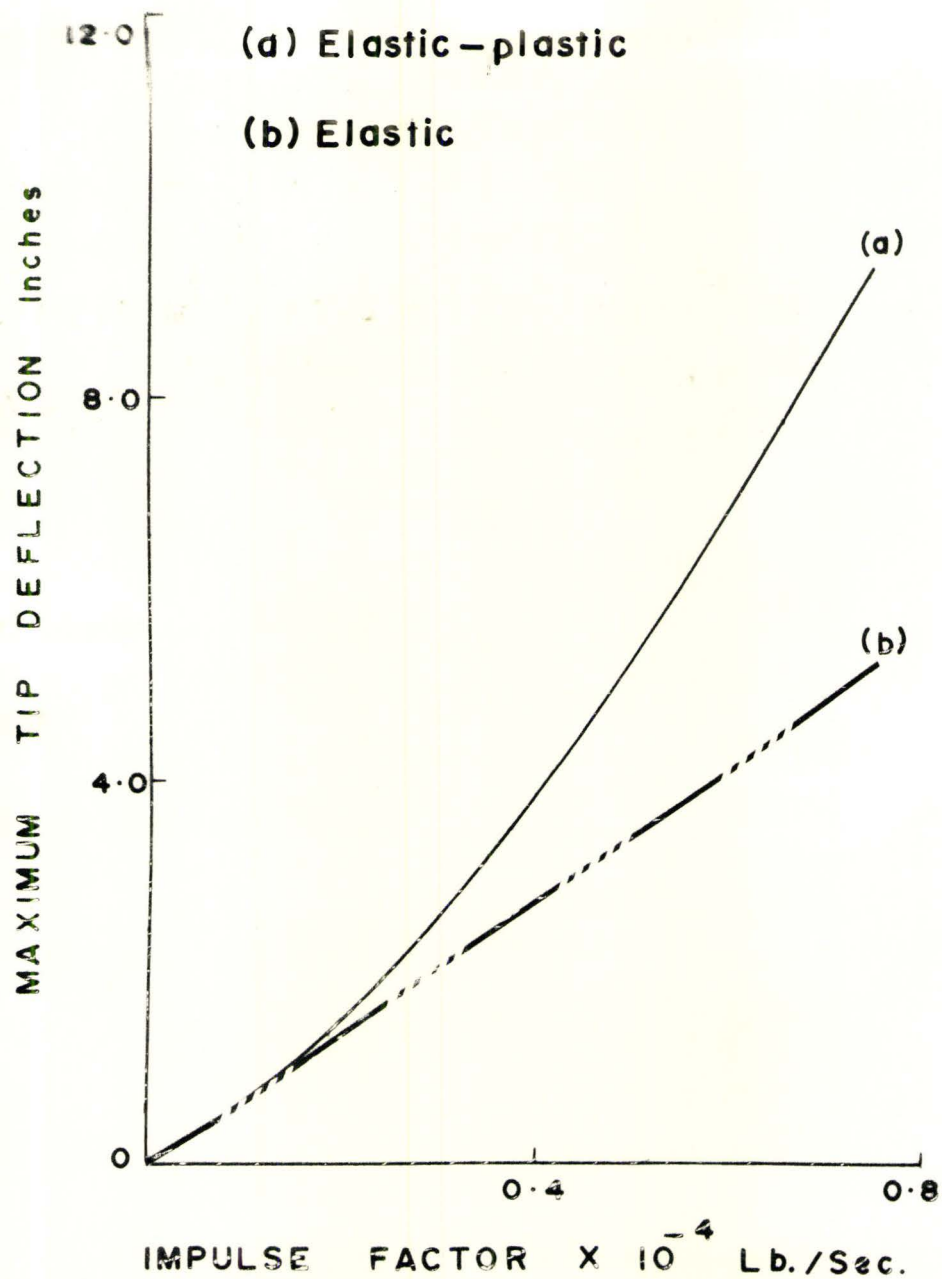
Figure 3.14   Impulse Factor versus Maximum Elastic-plastic and Elastic
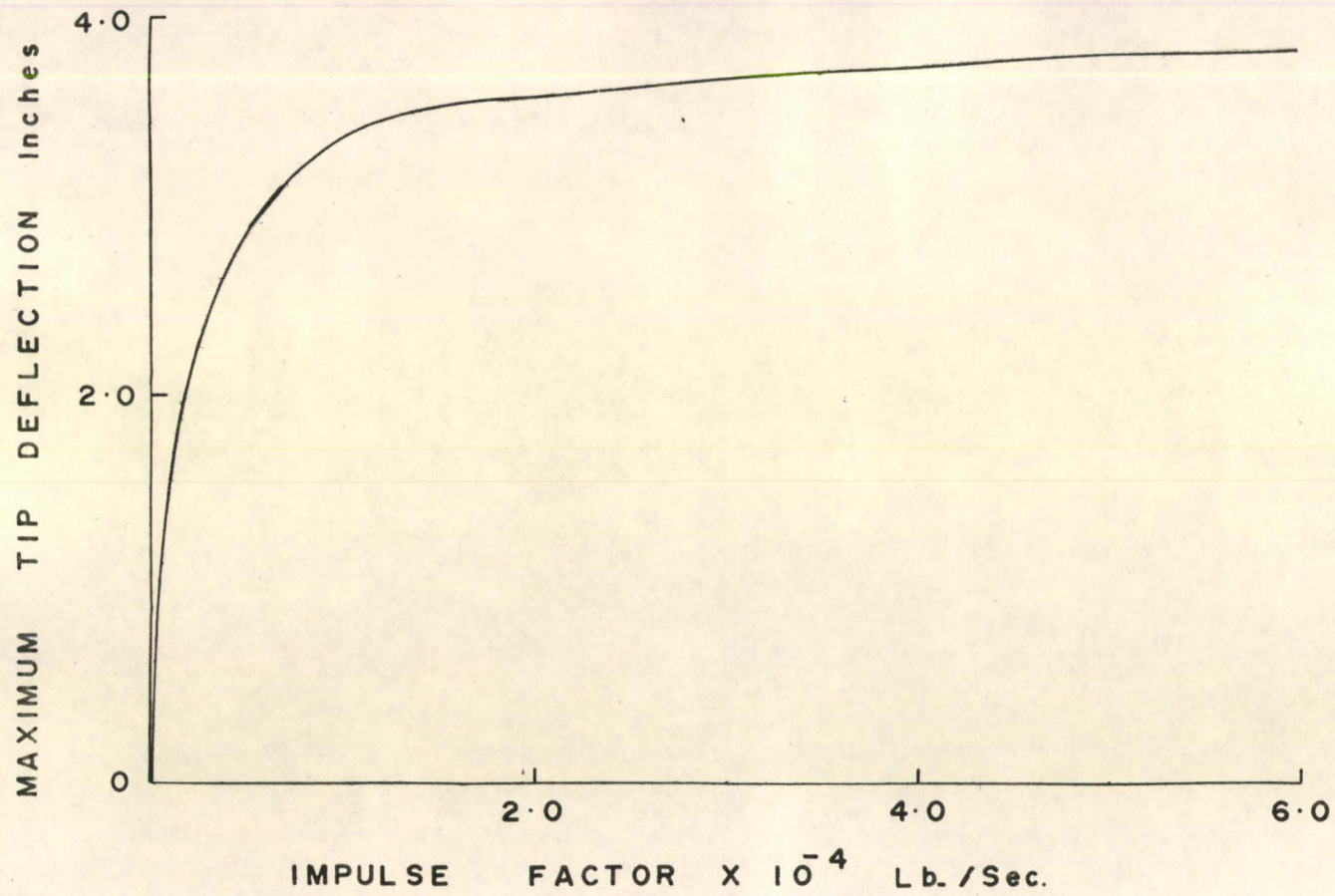Tip Deflections for Equal Pulse Duration - Series A

Also the time at which maximum tip deflection occurs is reduced with a decrease in pulse duration. Figs. 3.8 and 3.9 reveal a more realistic picture of the increase of maximum tip deflection, which increases more rapidly for lower values of impulse factor as compared to the higher values of impulse factor. Thus for lower values of impulse factor, the pulse duration has a significant effect on the maximum tip deflection, while for higher values of impulse factor the pulse duration does not have a significant effect on the maximum deflection. The low and high impulse factors are as defined in section 3.4 (2).

For the pulse of equal duration, the maximum and permanent tip deflections increase as area of the pulse increases.

The elastic-plastic beam shapes show the concentration of the curvature near the root, while for the purely elastic beam shapes the curvature is distributed along the entire length of the beam.

2) **Series B**

All the beams analysed in this series had the following properties:

Length	25 ft.
Cross-section	8" x 6 1/2" WF
Total weight	700 lbs.
Yield moment	81300 ft. lb.
Modulus of Elasticity	30×10^6 p.s.i.
Damping factor as percentage of critical damping coefficient	12.0

Approximated by 4 masses

These beams were also subjected to a symmetrical triangular pulse at the tip.

Table 3.3 gives a summary of the results for the elastic-plastic and elastic responses of these beams for constant pulse area. Figs. 3.15 to 3.20 show the graphical representation of these results.

Discussion of Series B

The response of the beams in this series for constant pulse area does not change as much with the change of duration as that of Series A. Thus here the response mainly depends on the area of the pulse. This can also be seen from Fig. 3.19 and 3.20. The values of the impulse factors for these beams lie in a range where the maximum tip deflection almost becomes constant. These values of impulse factors are high. On the other hand, low impulse factors are those for which the response of the beam changes significantly with change of duration, keeping pulse area constant.

At this stage it is rather difficult to set a definite limit for the low and high impulse factors. The impulse factor which is high for the beams of Series A will be considered low for the Series B beams. The properties of the beam play an important part in determining whether the impulse factor is high or low. Thus the high or low impulse factor is a relative term and will vary from beam to beam. For the purpose of the present investigation the high and low impulse factors will be taken as defined in the previous paragraph.

Beam No.	Pulse Area	Pulse Duration	Maximum Elastic-plastic Tip Deflection	Maximum Elastic Tip Deflection	Permanent Tip Deflection Corresponding to Column 4	Plastic Hinge Rotation at Root Corresponding to Column 4	Impulse Factor $\times 10^{-6}$
	lb.sec.	sec.	in.	in.	in.	radians	lb./sec.
1	2	3	4	5	6	7	8
B1	400.0	0.01	22.21	18.52	15.3	0.048	16.0
B2	400.0	0.02	21.47	18.39	14.7	0.05	4.0
B3	400.0	0.04	20.26	17.98	12.2	0.041	1.0

Table 3.3: Elastic-plastic and Elastic Response of Beams for Constant Pulse Area - Series B
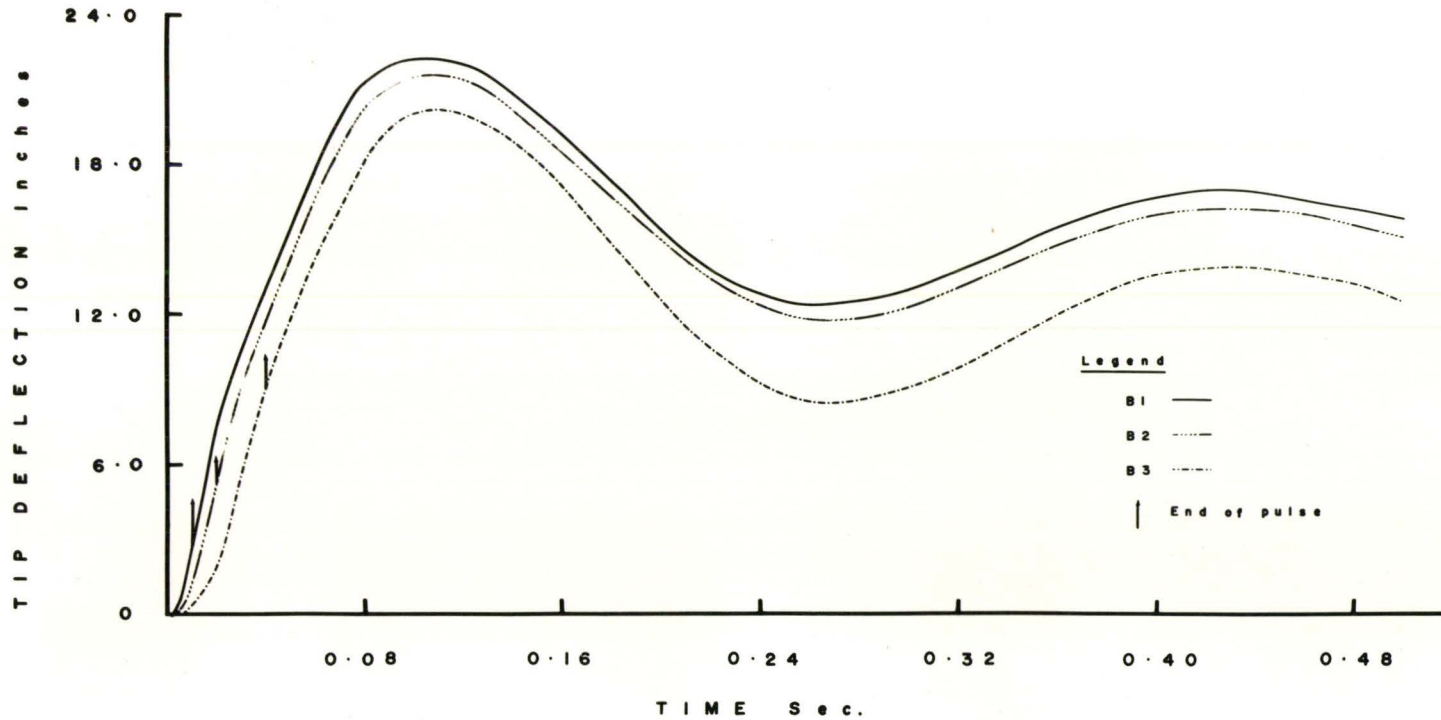
Figure 3.15 Elastic-plastic Response for Equal Pulse Area - Series B
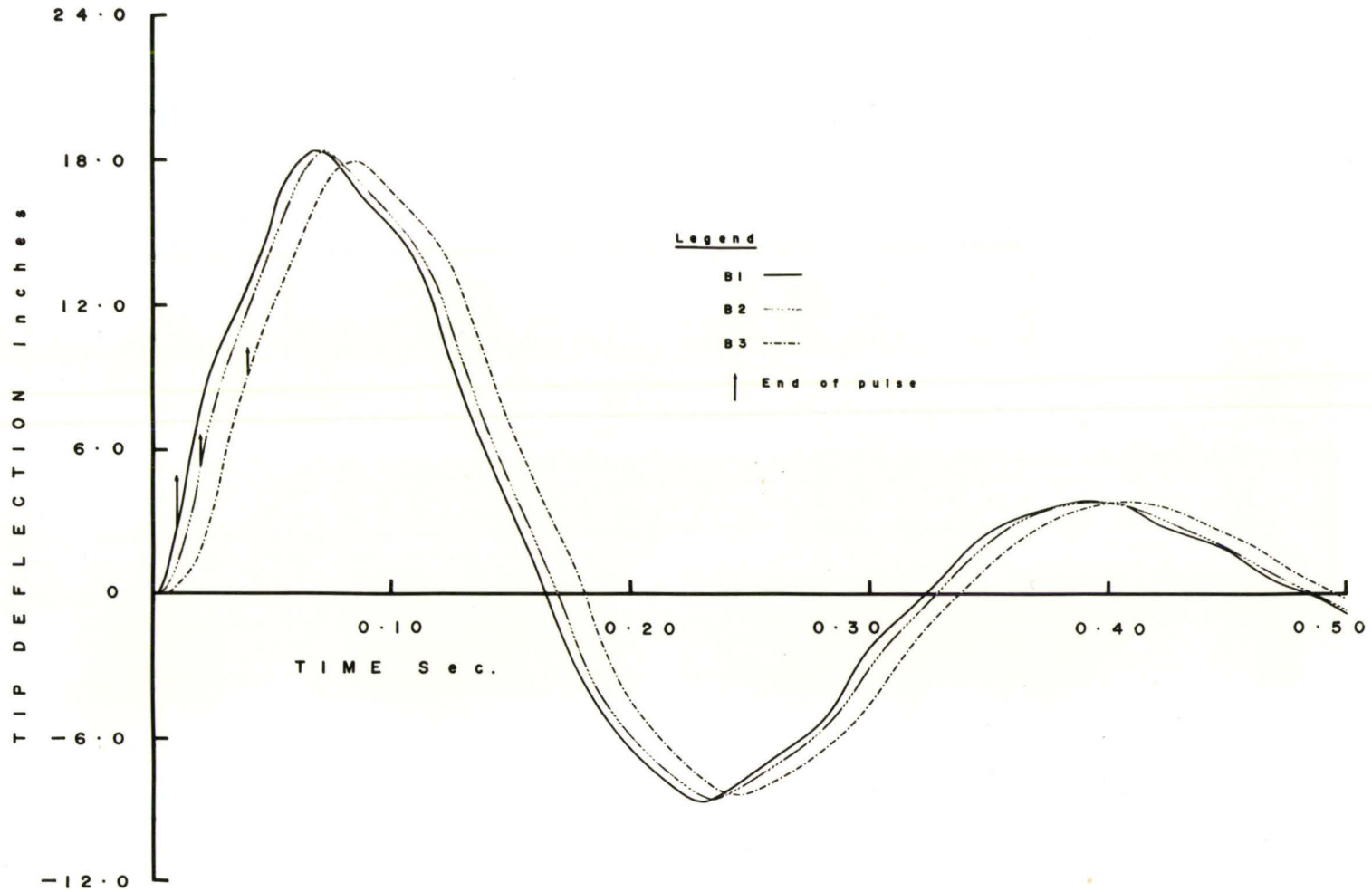
Figure 3.16 Elastic Response for Equal Pulse Area – Series B
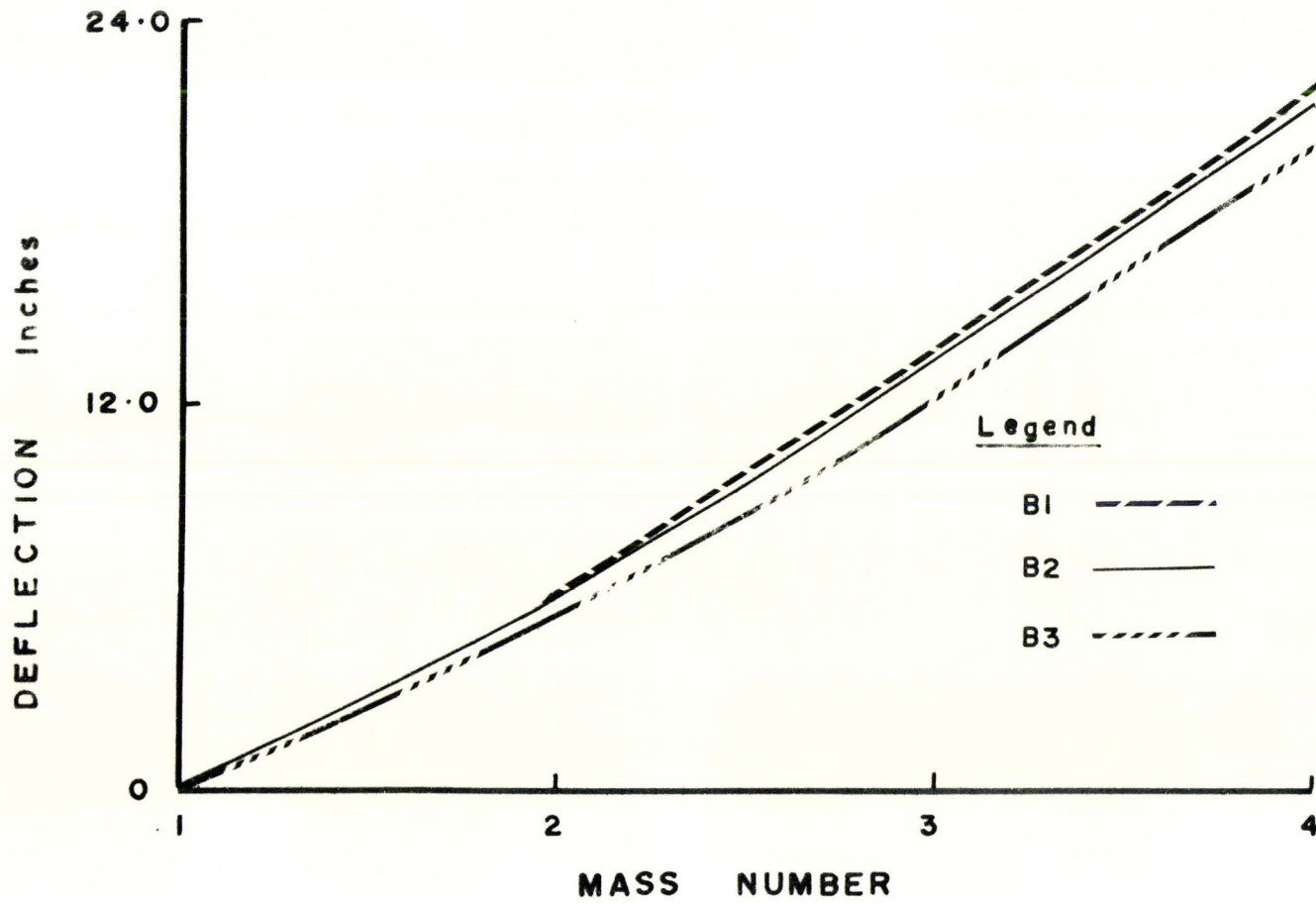
Figure 3.17 Elastic-plastic Beam Shapes at Maximum Tip Deflection for Equal Pulse Area – Series B
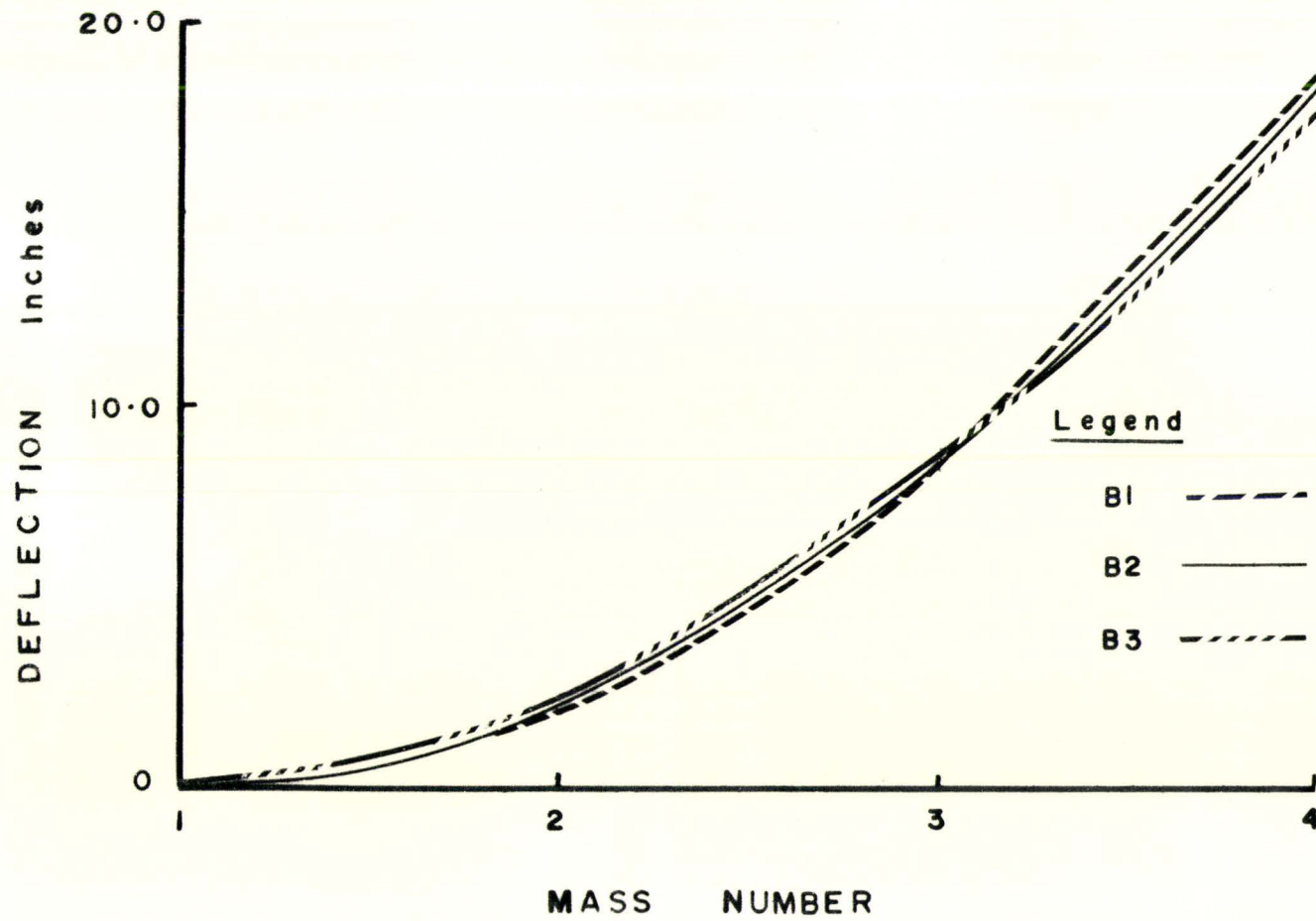
Figure 3.18 Elastic Beam Shapes at Maximum Tip Deflection for Equal Pulse Area - Series B
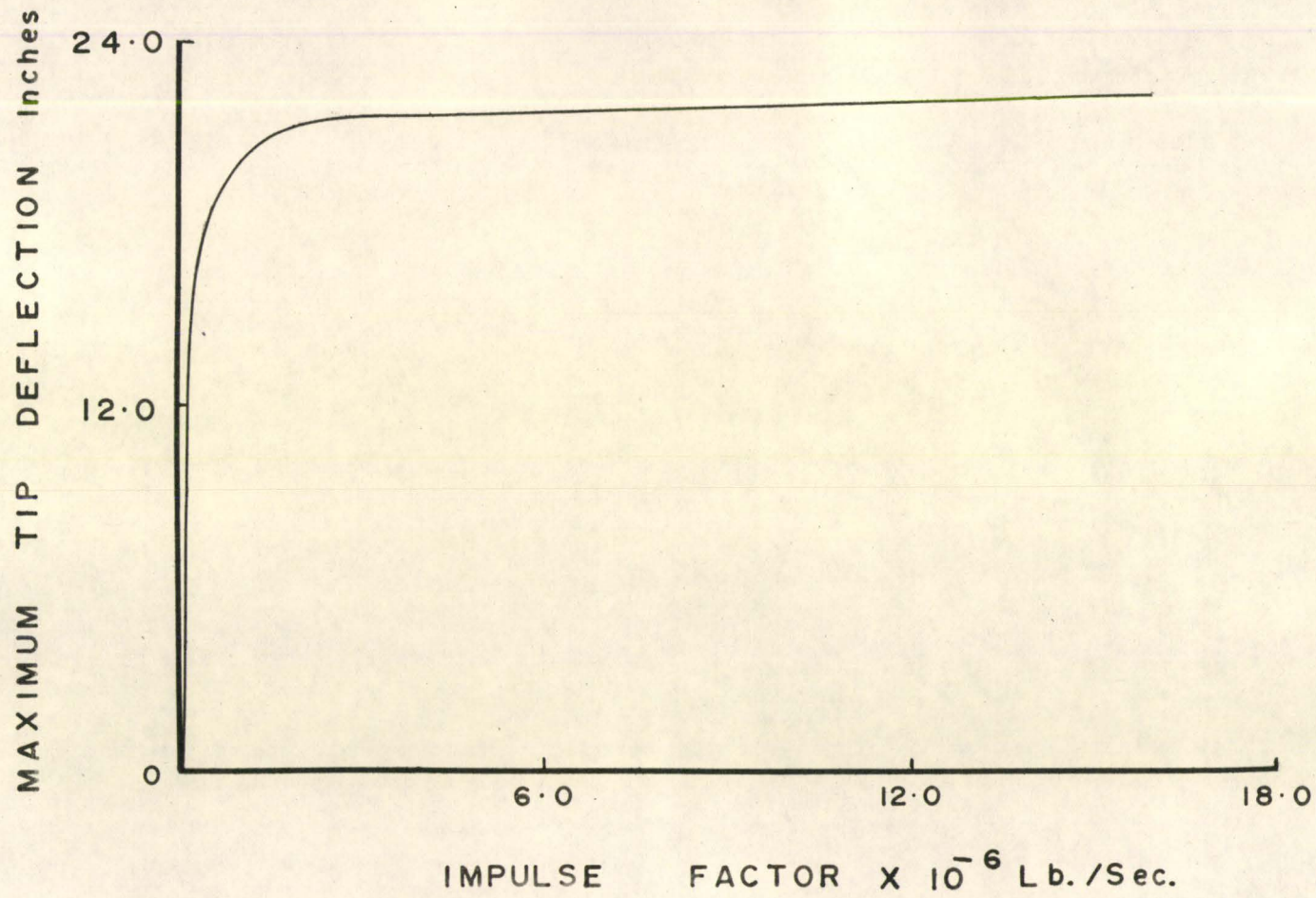
Figure 3.19   Impulse Factor versus Maximum Elastic-plastic Tip Deflection for Equal Pulse Area - Series B
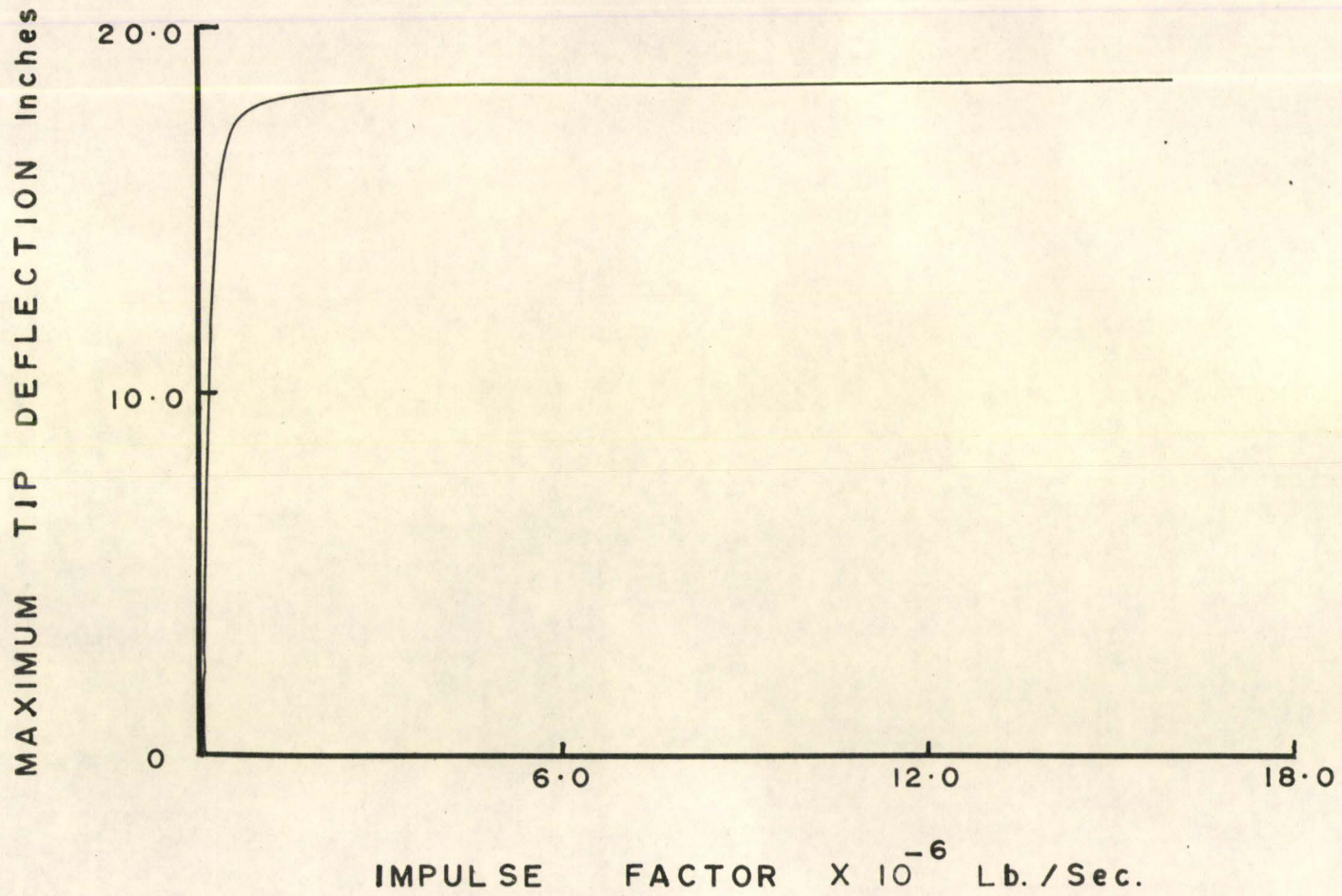
Figure 3.20   Impulse Factor versus Maximum Elastic Tip Deflection for Equal Pulse Area – Series B

Thus for beams of Series A the impulse factors which are greater than 10^4 lb./sec. are high, while for Series B values of impulse factors greater than 10^6 lb./sec. are considered high.

3) Series C

It was decided to analyse a few of the beams which Parkes[1] analysed in his paper. He analysed cantilever beams of various lengths, which were struck at the tip either by heavy or by light strikers. A heavy striker is a weight falling through a small height, and having a mass which is of the same order of magnitude as the mass of the beam. The heavy strikers used by Parkes rested on the beam after impact. Rifle bullets were used as light strikers, whose masses were small in comparison with those of the beams. The light strikers used by Parkes remained embedded in the beam after striking it.

Owing to the incomplete information available from Parkes' paper, some data had to be assumed. This included damping and duration of the pulse. The damping factor used was the same as determined during the experimental investigation described in this thesis (Section 4.4, Chapter IV). However it appeared rather difficult to assign a value to the pulse duration for the beams analysed by Parkes. This was because of the fact that the final deformation of the beam depended somewhat on the pulse duration, once the area of the pulse was fixed. This was more important for the heavy striker, where the duration of the pulse had a tendency to be longer. Therefore an arbitrary value was used for the pulse duration.

This value was greater for heavy striker as compared to that for light strikers. This was on account of the fact that light strikers struck the beam with a very high velocity (970 and 1580 ft./sec.) as compared to the lower velocity (6.4 to 18 ft./sec.) of the heavy strikers.

Three beams were chosen from Parkers' paper for the response analysis, two (C20 and C24) from the light strikers category and one (C4) from the category of the heave strikers. In order to include the strain rate effect, Parkes multiplied the static yield moment by various factors, to obtain the dynamic plastic moment. The same factors were used in this analysis. The properties of the beam included the following:

Length	12"
Cross-section	1/4" x 1/4"
Total weight	0.22 lbs.
Static yield moment	16.25 ft. lb.
Modulus of Elasticity	30×10^6 p.s.i.
Damping factor as percentage of critical damping coefficient	0.622

Approximated by 5 masses.

Further analytical data is given in Table 3.4. Pulse area was taken equal to the total momentum of the striker.

Discussion of Series C

In Table 3.5 comparisons are made between the results of this analysis and those obtained by Parkes. Parkes did not give values of the

Beam No.	Category	Pulse Area lb.sec.	Pulse Duration sec.	Factor on Static Moment	Maximum Tip Deflection in.	Permanent Tip Deflection in.	Plastic Hinge Rotation at Root radians	Impulse Factor $\times 10^{-4}$ lb./sec.
C4	Heavy Striker	0.8	0.05	1.5	4.54	3.2	0.267	0.128
C20	Light Striker	0.1302	0.006	1.6	1.95	0.77	0.064	1.45
C24	"	0.2474	0.01	1.7	4.18	2.88	0.24	0.99

Table 3.4: Elastic-plastic Response of Beams - Series C

Beam No.	Author's Analysis		Parkes' Analysis	
	Hinge Angle at the Root radians	Permanent Tip Deflection in.	Hinge Angle at the Root radians	Permanent Tip Deflection in.
C4	0.267	3.2	-	1.48
C20	0.064	0.77	0.06	-
C24	0.24	2.88	0.22	-

Table 3.5: Comparison of Parkes' and Author's Analytical Results

permanent tip deflections for beams struck by light strikers and the values of the hinge angle at the root for beams struck by heavy strikers.

It is evident from Table 3.5 that the results obtained for beams C20 and C24 compare favourably with those obtained by Parkes. There is not good agreement for beam C4. This is mainly due to the assumed value of the pulse duration, which is relatively important for beams hit by heavy strikers. This is again due to the fact that the impulse factor for the beam struck by a heavy striker is much lower than that for a beam hit by a light striker.

Very good agreement with Parkes' results should not be expected, as both his heavy and light strikers became part of the beam on impact. The results obtained for Parkes' beams using the analysis presented in this thesis, are for a pulse which ceases to act after a certain time.

The beam shapes at maximum tip deflection are shown in Fig. 3.21. These resemble the beam shapes of Fig. 3.6.
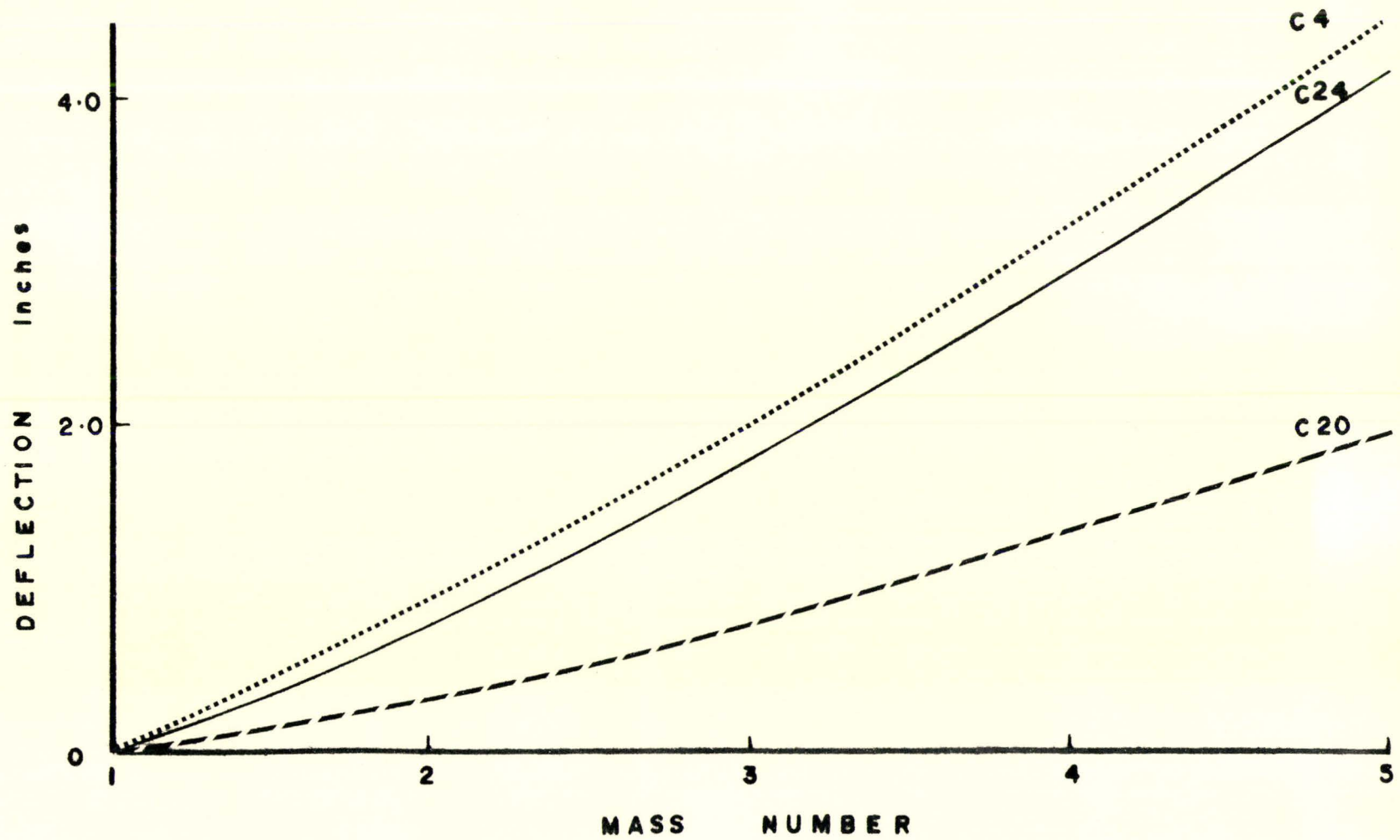
Figure 3.21   Elastic-plastic Beam Shapes at Maximum Tip Deflection - Series C

CHAPTER IV

Experimental Program

4.1 Description of the Equipment

The equipment used for the experimental work is shown in Figs.
4.1 and 4.2. It consists of a gravity force container A, which is a
16 ft. high tube with an inside diameter of 13.5 in. Tube A supports
a frame B, which in turn acts as a support for rocker arm C. A load
cell L is fixed on the rocker arm C as shown in Fig. 4.2.

A bucket, having 12.75 in. outside diameter, is put inside the
tube A. The weight of the bucket can be adjusted by using lead slabs.
The bucket can be hoisted up by means of a pulley, and can rest on a
pin P at a number of heights inside tube A. This pin is unscrewed
manually to release the bucket.

D is a frame fixed to the ground. Frame D acts as a support for
the beam support S. R is the recorder used for strain and load measure-
ments.

4.2 Beam Specimen

All the beams tested were 1/2" x 1/2" x 3' long and were cut from
the same material. This was done to ensure that the test specimen will
have the same material properties. Two sets of beams were tested. Each
set consisted of two beams. The typical beams tested in set D and set E
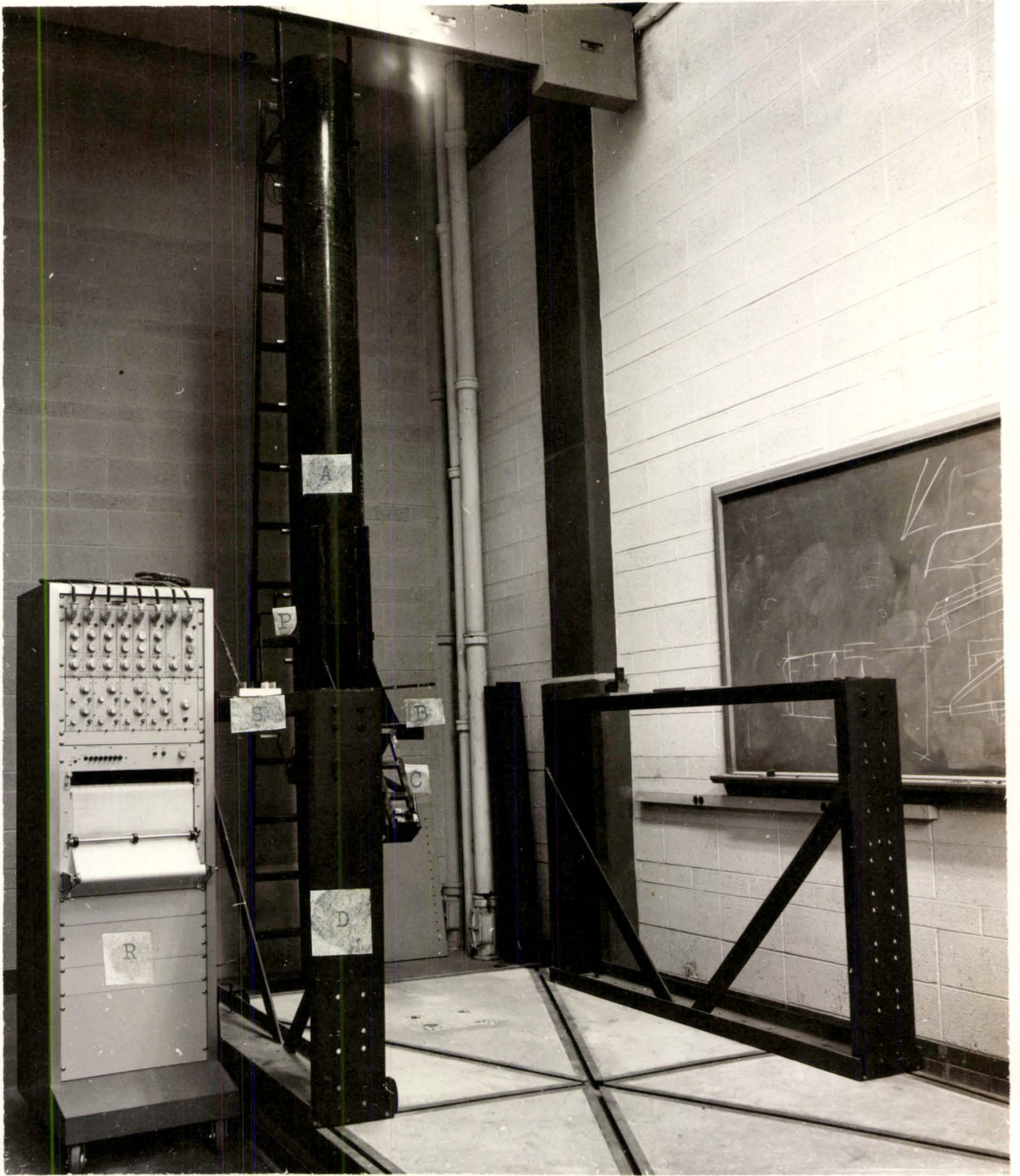
Figure 4.1   Experimental Equipment
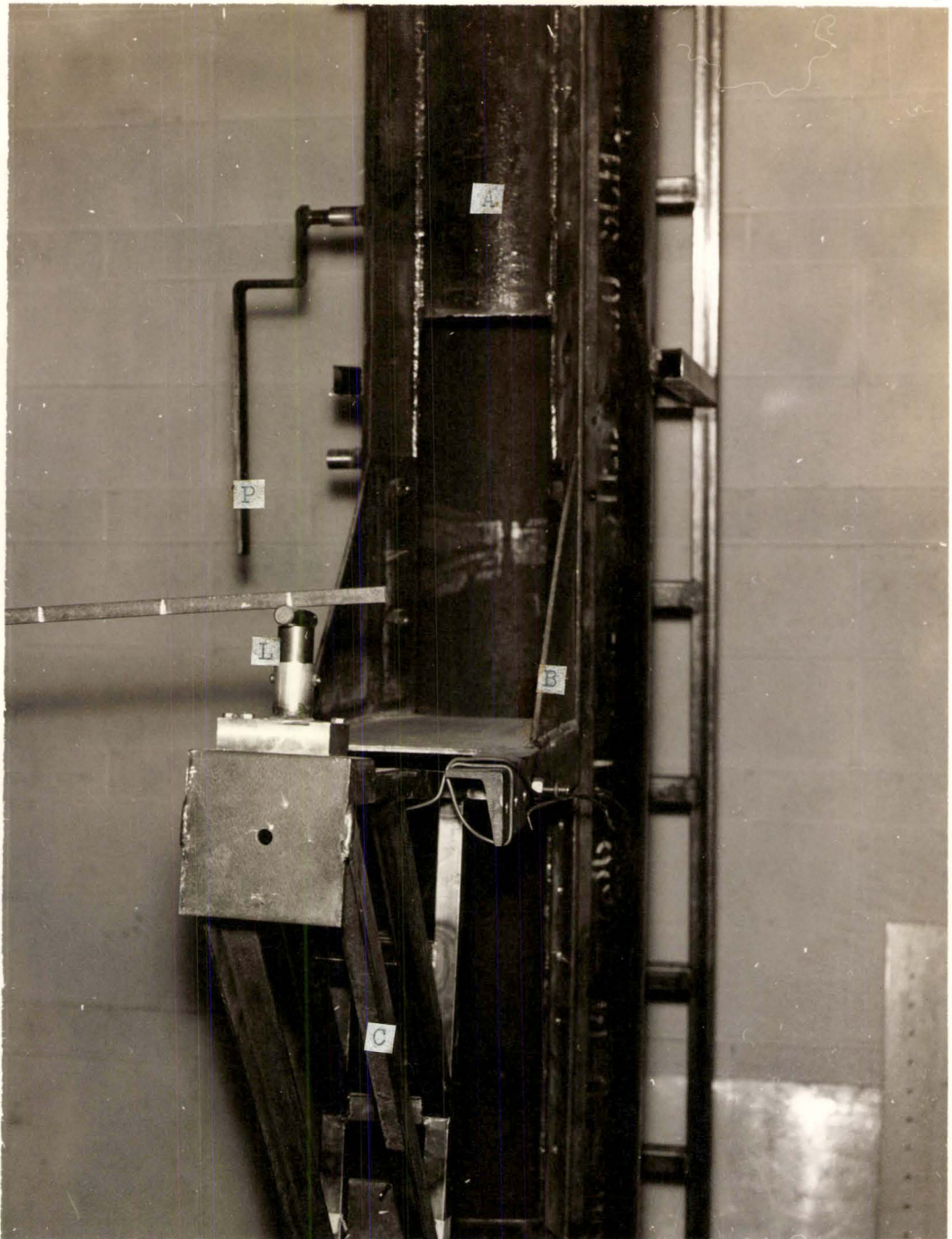
Figure 4.2 Experimental Equipment

are detailed in Fig. 4.3. Five high elongation strain gages were put on each beam in order to obtain a qualitative time record of strain measurements, and to obtain information about plastic and residual strains. The locations of strain gages for beams of set D were different than those for set E.

The beams had an effective length of 27 7/8". An overhang of 1 1/4" was given beyond the point of impact, as shown in Fig. 4.3. The remaining length of the beam was fixed in the support.

4.3 Calibration

(a) Strain Gages

To calibrate the strain gages, a static load of 25 lbs. was applied at the tip of the beam and the strain readings at all the gages were recorded by the recorder. On this basis a calibration table for various sensitivities was prepared.

(b) Load Cell

The load cell consisted of a tube whose outside and inside diameters were 1/2" and 1/4" respectively. The tube had four high elongation strain gages, equally spaced around the circumference.

The load cell was given a number of load cycles from 0 to 600 lbs. on a Tinus-Olsen testing machine. This was done in order to reach a stage where the load deformation characteristics did not change appreciably.
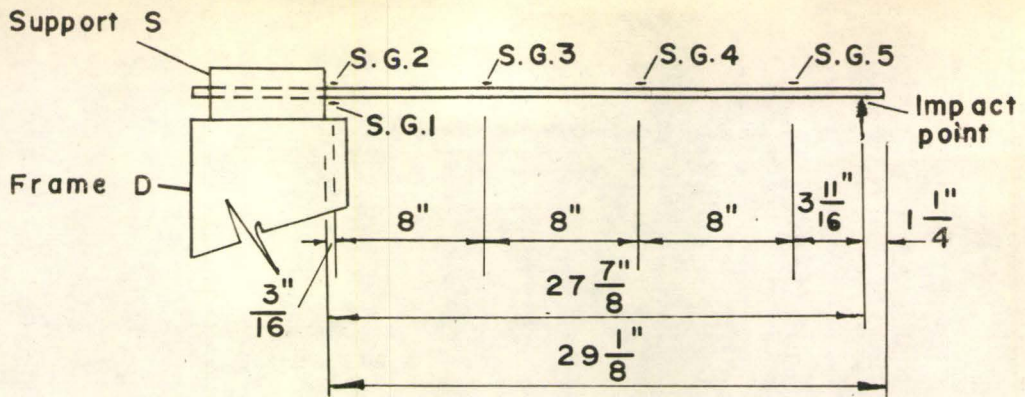
Typical beam of Set E

Legend

Cross—section	1/2" x 1/2"
Total weight	2·06 lbs.
Modulus of Elasticity	30×10^6 p.s.i.
Static yield moment	104·2 ft. lb.
Damping factor (% of critical damping)	0·622

S.G. stands for strain gage.
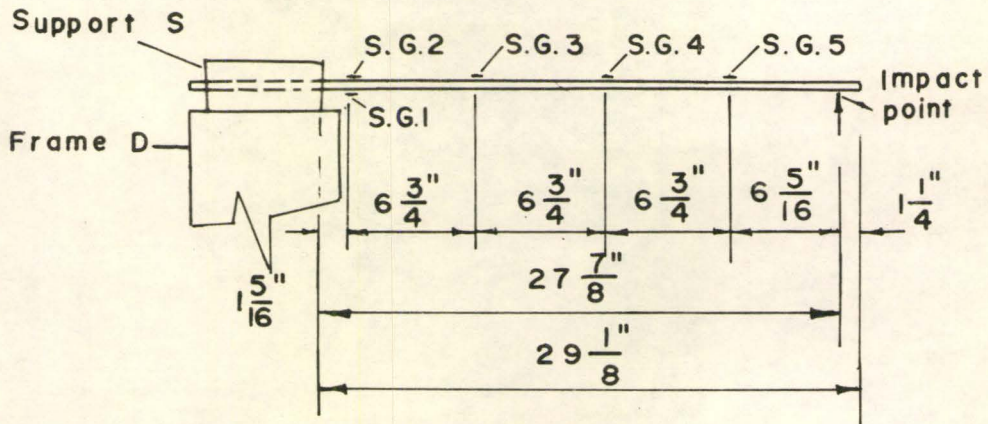
Typical beam of Set D

Figure 4.3 Details of Typical Experimental Beams

The load cell was connected to the recorder, and was loaded upto various load levels for different sensitivities. The calibration table was then prepared.

4.4 Damping

The strain recordings for the free vibration of the beam were taken and were plotted on a semi-log scale to find the damping factor. This plot showed that the damping in the system was approximately viscous. The value of the damping factor was found to be 0.00622.

4.5 Tensile Tests

Two tensile test coupons were prepared from additional lengths of the same material as the material of the beam specimens.

Tensile tests were conducted to obtain the yield point of the steel used. The average yield stress obtained was 40,000 p.s.i.

4.6 Testing Procedure

The bucket having the desired amount of weight was dropped from the required height. It struck the rocker arm C, which in turn struck the beam specimen from below as shown in Fig. 4.2. The rocker arm fell back under gravity after striking the beam. This was done to minimize the inertial contact between the striker and the beam specimen.

The recorder was put on just before the bucket was dropped. All the strain recordings during the experiment were done at a paper speed of 5 cm/sec.

The final deflections of the strain gage points and the tip of the beam were taken by a theodolite.

CHAPTER V

Experimental Results

5.1 Test Results

Four beams were tested in this investigation. The tests were carried out for various combinations of the bucket height and weight. Other details and results are as given in Table 5.1. Typical record of strains and load, measured during the experiment, are shown in Figs. 5.1 and 5.2 respectively.

5.2 Conclusions from Experimental Results

The four beams tested were subjected to pulses of low impulse factors. As predicted by analytical results, the permanent tip deflections of these beams should depend mainly on pulse area. This is evident from the results of Table 5.1.

The permanently deformed beams had some curvature at the root. As expected this was more pronounced for the beams of Set E, which were subjected to a pulse of greater area. The remaining portion of the beam was almost straight and thus resembled the shape of the analytical curves in Fig. 3.6.

5.3 Deflection Calculations from Experimental Record

Attempts were made to calculate the deflections and plastic hinge rotations from experimental strain records. The value of the permanent

Beam No.	Height of Bucket ft.	Weight of Bucket lbs.	Pulse Duration		Pulse Area lb.sec.	Impulse Factor x 10^{-4} lb./sec.	Permanent Deflection of Impact Point of the Beam in.
			T_1 sec.	T_2 sec.			
D1	2.0	125	0.02	0.05	1.6	0.13	0.76
D2	2.0	150	0.02	0.06	2.08	0.13	1.33
E1	3.0	125	0.03	0.15	5.04	0.062	3.3
E2	3.0	150	0.04	0.14	6.81	0.083	4.0

Table 5.1: Experimental Results

S.G.2 , 1900 micro in. per in. per cm.

S.G.3 , 950 micro in. per in. per cm.

S.G.4 , 475 micro in. per in. per cm.

S.G.5 , 95 micro in. per in. per cm.

TIME sec.
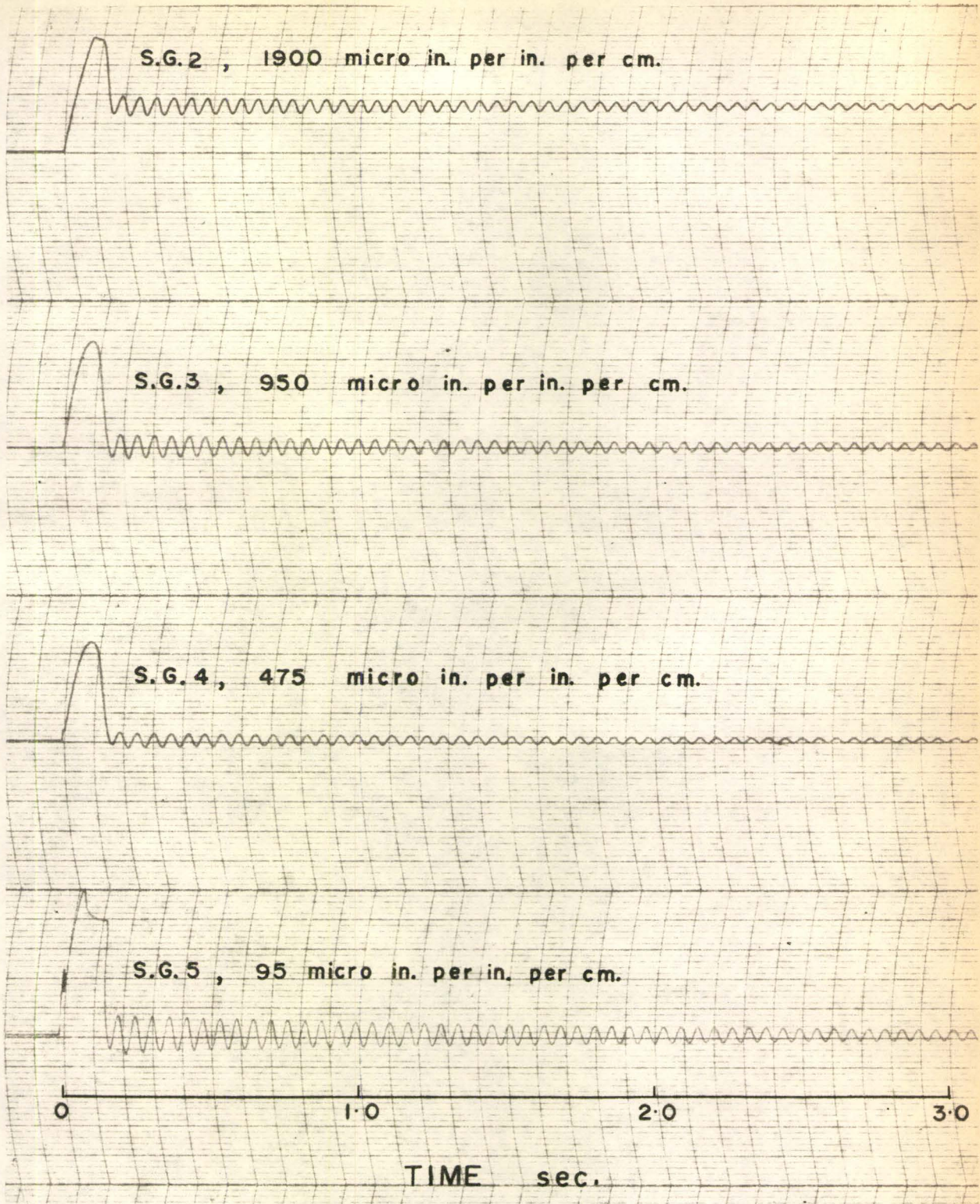
Figure 5.1 Typical Experimental Strain Record

a to b   Bucket hits Rocker arm

b to c   Rocker arm moving to hit the beam

c to d   Contact of Rocker arm and the beam

d to e   Rocker arm falls under gravity and hits the tube A
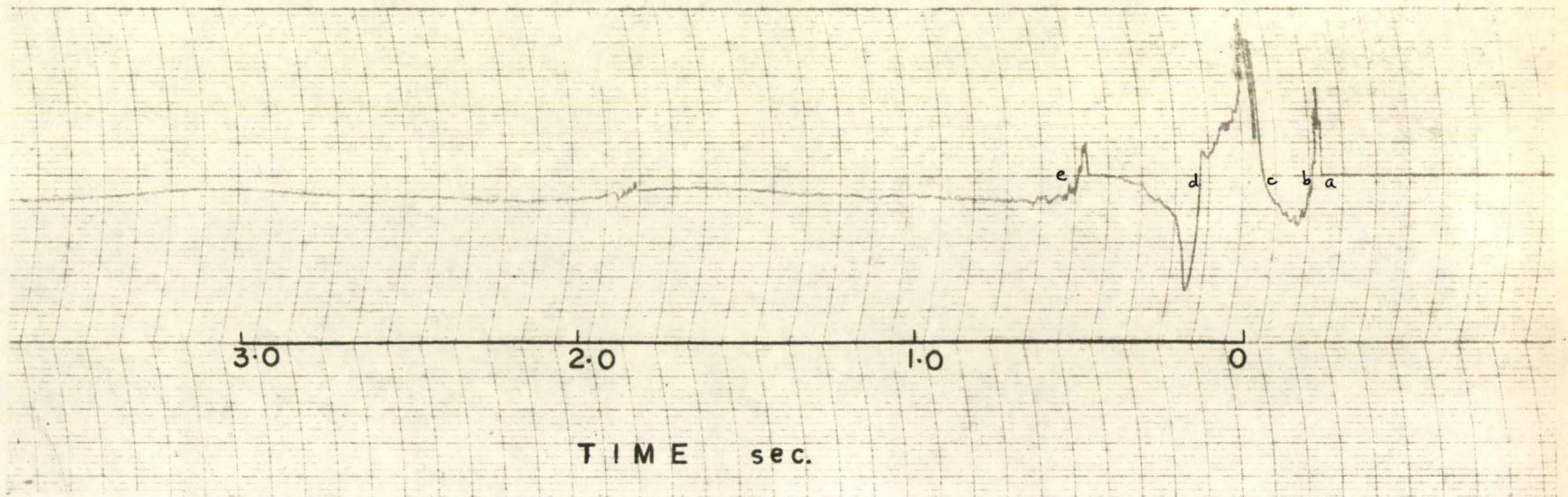
Figure 5.2 Typical Experimental Load Record

deflection calculated through these records was 23% lower than that observed by the theodolite. This discrepancy could be due to the fact that there was no strain gage exactly at the root of the beam and so the strain at the root was not known.

5.4 Strain Rate

The strain rate determined from the experimental records for the beams tested was approximately 0.1 in/in per sec. As shown by Manjoine[2], the yield stress for a strain rate of 0.1 in/in per sec. is 1.3 times the static yield stress. Thus a factor of 1.3 was used while calculating the dynamic yield moment.

5.5 Experimental Pulse

The experimental shape of the pulse obtained from the load record can be approximated by a triangle as shown in Fig. 5.3. A similar shape was used while calculating the response of these beams.

5.6 Simulation of Experimental Results on Computer

The analysis developed in Chapter II was used to find the response of the beams tested. The data used is shown below:

Length	27-7/8 in.
Total weight	1.98 lb.
Static yield moment	104.2 ft. lb.
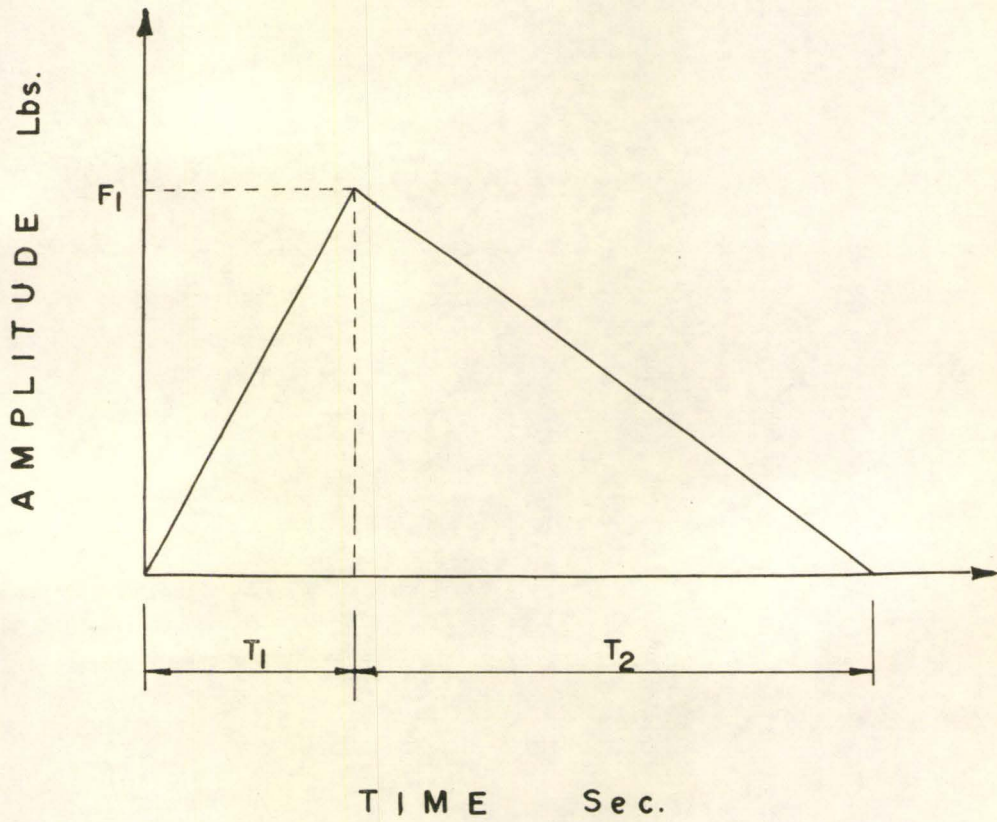
Figure 5.3 Approximate Shape of Experimental Pulse Record

Dynamic yield moment   1.3 x 104.2 = 135.5 ft. lb.

Modulus of Elasticity 30×10^6 p.s.i.

Damping factor as percentage   0.622
of critical damping coefficient

Approximated by 5 masses.

Table 5.2 gives the properties of the pulse applied and the
results obtained.

5.7 Comparison of Analytical and Experimental Results

As may be seen from the results shown in Tables 5.1 and 5.2, the
experimental results are much lower than those obtained theoretically.
It is only for beam E_1 that experimentally and theoretically determined
values of permanent deflections agree.

The principal cause for this difference was the load measuring
device, which was found to be unreliable. The load cell was calibrated
after each impact test, and each time it showed a different load modulus
(lb. per unit recorder displacement), which also varied for different
sensitivities of the recorder. Also the load cell record showed some
residual strain after every test, as seen in the typical load cell record
in Fig. 5.2

It is also believed that there was a considerable amount of strain
hardening at the root of the specimen, especially in case of beams E_1
and E_2. For these beams strain gages 1 and 2 recorded the maximum strain
of about 15 to 17 times the yield strain, which, according to Beedle[13],
is the strain hardening range.

Beam No.	Pulse Area	Pulse Duration		Impulse Factor x 10^{-4}	Maximum Tip Deflection	Permanent Tip Deflection	Plastic Hinge Rotation at the Root
		T_1	T_2				
	lb.sec.	sec.	sec.	lb./sec.	in.	in.	radians
D1	1.6	0.02	0.05	0.13	3.5	1.09	0.039
D2	2.03	0.02	0.06	0.13	4.55	2.1	0.075
E1	5.04	0.03	0.15	0.062	5.94	3.47	0.124
E2	6.81	0.04	0.14	0.083	20.4	17.9	0.64

Table 5.2: Analytical Results of Experimentally Tested Beams

The experimental beams were 1-1/4" longer (overhang beyond the impact point) than the analytical beams. This would also account for some of the differences in results.

A differential transformer was considered for taking deflection measurements during the experiment. However, it could not be used because of the large deflections and the relative rotation at the end.

CHAPTER VI

Conclusions and Suggestions

6.1 Analytical Results

The analytical results of the cantilever beams subjected to an impulse at the tip show that the response greatly depends on impulse factor. If the impulse factor is low, the response is governed both by the duration and area of the pulse. For a high impulse factor the response does not depend so much on the duration of the pulse.

The boundary between what can be considered as low or high impulse factor varies from beam to beam. In other words, the properties of the beam as well as that of the pulse are to be taken into consideration for assigning low and high values to impulse factors. The results obtained in the present investigation are not sufficient to be able to predict this boundary for a beam of given properties. However, on the basis of the results obtained, low and high impulse factors for a constant area pulse may be defined as follows:

"For low impuse factors, the maximum and permanent tip deflections depend mainly on the duration of the pulse. For high impulse factors these are almost independent of the duration. For very high values of impulse factors the maximum and permanent deflections tend to be asymptotic to a certain constant value."

On this basis the impulse factors higher than 10^4 and 10^6 lb./sec. are considered high for beams of series A and B respectively.

It was observed during the analysis of series A that for those beams whose impulse factors are higher than 10^4 lb/sec., the first plastic hinge was formed closer to the tip and moved gradually towards the root, where it stayed until the whole system returned to the elastic state. For beams having impulse factors lower than 10^4 lb/sec. the first plastic hinge was formed closer to or at the root.

In series B, it was only for beam B_1 (which has the highest impulse factor of that series) in which the first hinge was formed near the tip and travelled towards the root. For other beams of this series the first hinge was always formed at the root.

The beams which Parkes analysed for light and heavy strikers were also analysed by the analysis presented in this thesis. A close agreement was observed between the results, for the beams hit by light strikers. The agreement was not very good for heavy strikers category. This may be mainly due to the assumed value of the pulse duration, which is important for beams hit by heavy strikers as their impulse factors are low.

The other reason for this difference is that the Parkes' light and heavy strikers rested on the beam after striking it. On the other hand, the analysis done in this thesis for Parkes' beams was for a pulse, which only acts for a particular duration.

6.2 Experimental Results

The experimental results showed that for beams of low impulse factors, permanent tip deflections depend mainly on the pulse area.

Also the permanently deformed beams had some curvature near the root and the deformed shapes compared favorably with those computed by the analytical method.

The agreement between the experimental and analytical results for the same beam is only fair. The analytical results are higher than those observed experimentally. A better agreement could not be expected. This is chiefly because of the load measuring device, which yielded unreliable results.

The other reason for this discrepancy is believed to be the strain hardening effect at the root, where the strains were more than 15 to 17 times the yield strain.

6.3 Suggestions for Further Research

(a) Analytical Work

As mentioned in the conclusions, the investigation presented herein is insufficient to assign general values for high and low impulse factors. Further research is necessary for determining these values.

A number of series of beams may be analysed for various pulses. Each series should consist of beams having the same elastic-plastic properties but of different lengths.

Pulses applied should include a number of triangular pulses having constant areas, with different durations.

These results would provide better information regarding the behaviour of the beams with respect to impulse factors. It is expected that the properties of the beam would play an important role in determining high and low impulse factors.

(b)   Improvements in the Equipment

The equipment used for the experimental work was by no means sophisticated. It needs a number of refinements before it can be relied upon for satisfactory results.

The most important of all is a much better and more accurate load measuring device whose calibration should be reproducible at any time. This will ensure a better comparison between analytical and experimental results.

Deflection measurements during the test are necessary to plot the beam shape at any instance, which can be compared to the analytical shape. This will also eliminate the use of the theodolite for measuring the permanent deflection of the beam.

The duration of the pulse obtained from experimental records was quite long as compared to the fundamental period of the beam. There was no way of controlling the duration to a desired limit. Some catch arrangement is suggested for limiting this duration. It would make possible the equal duration pulses with various areas to be applied to the beams.

The bucket could not be dropped from a height of more than 3 ft. as it would have required an overhang of about 3 in. beyond the point of impact. Without this overhang the rocker arm after hitting the beam would go higher and would rest on the beam while falling.

A catch arrangement, which would restrict the rocker arm from going beyond a certain limit is required for this purpose also. Thus a catch arrangement would solve two purposes. In this way more combinations of bucket height and bucket weight will be available.

Another improvement in the equipment may be an electrical device for releasing the bucket. It would be better still if the bucket releasing device is connected to the recorder, so that the bucket falls as soon as the recorder is put on. This will also eliminate the trouble and time taken in unscrewing the pin manually for releasing the bucket.

APPENDIX

Complete Derivation of Resistance Matrices

Let ϕ_i be expressed as

$$\phi_i = X_i + \Psi_i \tag{A-1}$$

where X_i is the variable part of the plastic hinge rotation and Ψ_i is the constant part of the plastic hinge rotation due to the residual plastic deformation.

It is convenient to define the non-dimensional form of the following quantities

$$[\overline{P}] = \frac{1}{\lambda} [P]$$

$$[\overline{Q}] = \frac{EI}{\lambda^2} [Q]$$

$$\{\overline{M}\} = \frac{\lambda}{EI} \{M\} \tag{A-2}$$

$$\{\overline{U}\} = \frac{1}{\lambda} \{U\}$$

$$\{\overline{X}\} = \{X\}$$

$$\{\overline{\Psi}\} = \{\Psi\}$$

Substituting Eqs. A-1 and A-2 in the Eq. 2.3 yields the following

$$\{\overline{U}\} = [\overline{P}] \{\overline{X}\} + [\overline{P}] \{\overline{\Psi}\} + [\overline{Q}]\{\overline{M}\} \tag{A-3}$$

Noting that $\{\overline{\Psi}\}$ are the residual plastic hinge rotations which are constant at any given time, one may write

$$\{\overline{H}\} = [\overline{P}] \{\overline{\Psi}\} \tag{A-4}$$

- 73 -

from which

$$\{\overline{U}\} = \{\overline{H}\} + [\overline{P}] \{\overline{X}\} + [\overline{Q}]\{\overline{M}\} \tag{A-5}$$

Both $\overline{M}_i$ and $\overline{X}_i$ cannot be variable at the same time. At any mass-point, one is the variable while the other is a constant depending upon whether or not a plastic hinge exists at that point. It can be shown that Eq. A-5 can be written in the following form

$$\{\overline{U}\} = \{\overline{W}\} + [\overline{S}] \{\overline{Z}\} \tag{A-6}$$

where the elements of the matrix $[\overline{S}]$ and column vectors $\{\overline{W}\}$ and $\{\overline{Z}\}$ are defined by

$$\overline{W}_i = \overline{H}_i + \sum_{j=1}^{n} \Delta_j \overline{Q}_{ij} \overline{M}_j^* \tag{A-7}$$

$$\overline{S}_{ij} = (1 - \Delta^2 j) \overline{Q}_{ij} + \Delta_j^2 \overline{P}_{ij} \tag{A-8}$$

$$\overline{Z}_j = (1 - \Delta_j^2) \overline{M}_j + \Delta_j^2 \overline{X}_j \tag{A-9}$$

where Δ_j is defined as: $\Delta_j = + 1$ if mass-point j is plastic with a positive yield moment, $\Delta_j = 0$ if mass-point j is elastic, and $\Delta_j = -1$ is mass-point j is plastic with a negative yield moment; and $\overline{M}_j^*$ is defined by

$$\overline{M}_j^* = \frac{\lambda}{EI} M_j^* \tag{A-10}$$

Eq. A-6 is written in the above form to separate the variable quantities from the constants, with Eqs. A-7, A-8 and A-9 governing the separation conditions.

Pre-multiplying Eq. A-6 by the inverse of [S] and rearranging yields

$$\{\overline{Z}\} = - [\overline{S}]^{-1}\{\overline{W}\} + [\overline{S}]^{-1} \{\overline{U}\} \tag{A-11}$$

Note that column vector $\{\overline{W}\}$ is a set of constant values at any given time, one may write

$$\{\overline{G}\} = [S]^{-1} \{\overline{W}\} \tag{A-12}$$

Eq. A-11 may now be written as

$$\{\overline{Z}\} = [\overline{S}]^{-1} \{\overline{U}\} - \{\overline{G}\} \tag{A-13}$$

As $\{\overline{Z}\}$ is made up of a combination of portions of $\{\overline{M}\}$ and $\{\overline{X}\}$ it can be shown that Eq. A-13 yields, upon separation of variables, the following two equations

$$\{\overline{X}\} = [\overline{\Theta}]\{\overline{U}\} + \{\overline{\Gamma}\} \tag{A-14}$$

$$\{\overline{M}\} = [\overline{T}]\{\overline{U}\} + \{\overline{L}\} \tag{A-15}$$

The elements of the matrices in Eqs. A-14 and A-15 are defined as follows

$$\overline{\Theta}_{ij} = \Delta_i^{\,2} \, \overline{S}_{ij}^{\,-1} \tag{A-16}$$

$$\overline{\Gamma}_i = - \Delta_i^{\,2} \, \overline{G}_i \tag{A-17}$$

$$\overline{T}_{ij} = (1 - \Delta_i^{\,2}) \, \overline{S}_{ij}^{\,-1} \tag{A-18}$$

$$\overline{L}_i = -(1 - \Delta_i^2) \, \overline{G}_i + \Delta_i \, M_i^* \tag{A-19}$$

where $\overline{S}_{ij}^{\,-1}$ is the general element of $[\overline{S}]^{-1}$ and Δ_i is as defined previously. The second term of Eq. A-19 provides for either a positive or negative yield moment depending upon the sign of the plastic hinge rotation X_i.

Consider now the relationsip between the bending moments M_i and the resisting forces R_i. It can be shown by an equilibrium analysis of the original cantilever beam of Fig. 2.3a that the following holds true

$$\{M\} = \lambda \ [P^T] \ \{R\} \tag{A-20}$$

in which $[P^T]$ is the transpose of $[P]$.

Introducing the non-dimensional form of $\{R\}$

$$\{\overline{R}\} = \frac{\lambda^2}{EI} \ \{R\} \tag{A-21}$$

Eq. (A-20) takes the form

$$\{\overline{M}\} = [\overline{P}^T] \ \{\overline{R}\} \tag{A-22}$$

Pre-multiplying Eq. A-22 by $[\overline{P}^T]^{-1}$ yields

$$\{\overline{R}\} = [\overline{P}^T]^{-1} \ \{M\} \tag{A-23}$$

Substituting Eq. A-15 into Eq. (A-23) gives

$$\{\overline{R}\} = [\overline{P}^T]^{-1} \ [\overline{T}] \ \{\overline{U}\} \ + \ [\overline{P}^T]^{-1} \ \{\overline{L}\} \tag{A-24}$$

Let

$$[\overline{A}] = [\overline{P}^T]^{-1} \ [\overline{T}] \tag{A-25}$$

and

$$\{\overline{B}\} = [\overline{P}^T]^{-1} \ \{\overline{L}\} \tag{A-26}$$

Eq. A-24 can now be written as

$$\{\overline{R}\} = [\overline{A}] \ \{\overline{U}\} \ + \ \{\overline{B}\} \tag{A-27}$$

In order to calculate the actual forces from given dimensional deflections, Eq. A-27 can be written in the following form

$$\{R\} = [A] \ \{U\} + \ \{B\} \tag{A-28}$$

in which

$$[\Lambda] = \frac{\lambda^3}{EI} [\widehat{A}] \tag{A-29}$$

$$\{B\} = \frac{\lambda^2}{EI} \{\overline{B}\} \tag{A-30}$$

To compute bending moments, the dimensional form of Eq. A-15 may be used.

$$\{M\} = \frac{EI}{\lambda^2} [\overline{T}] \{\overline{U}\} + \frac{EI}{\lambda} \{\overline{L}\} \tag{A-31}$$

Plastic hinge rotations may be computed by using the dimensional form of Eq. A-14

$$\{X\} = \frac{1}{\lambda} [\widehat{Q}] \{\overline{U}\} + \{\overline{\Gamma}\} \tag{A-32}$$

Substituting Eq. A-32 into Eq. A-1 and making the substitution $\{K\} = \{\overline{\Gamma}\} + \{\overline{\Psi}\}$ yields

$$\{\phi\} = \frac{1}{\lambda} [\overline{Q}] \{\overline{U}\} + \{K\} \tag{A-33}$$

BIBLIOGRAPHY

1. Parkes, E.W., "The Permanent Deformation of a Cantilever Struck Transversely at its Tip", Proceedings of the Royal Society of London, England, Series A, Vol. 228, 1955, pp. 462-476.

2. Manjoine, M. J., "Influence of Rate of Strain and Temperature on Yield Stresses of Mild Steel", Journal of Applied Mechanics, Vol. 11, Trans., ASME, Vol. 66, 1944, p. 211.

3. Mentel, T.J., "The Plastic Deformation Due to Impact of a Canti- lever Beam with Attached Tip Mass", Journal of Applied Mechanics, Vol. 25, Trans., ASME, Vol. 80, 1958, p. 515.

4. Bodner, S.R., and Symonds, P.S., "Plastic Deformations in Impact and Impulsive Loading of Beams", Plasticity, Pergamon Press, London, England, 1960, p. 488.

5. Bodner, S.R. and Symonds,P.S., "Experimental and Theoretical Investigation of the Plastic Deformation of Cantilever Beams Subjected to Impulsive Loading", Journal of Applied Mechanics, December 1962, p. 719.

6. Schultz, A.B., "Nonlinear Response of Beams to Shock Pulse", Ph.D. Thesis, Yale University, 1962.

7. Schultz, A.B., "Nonlinear Response of a Beam to Shock Pulse," Journal, Franklin Institute, Vol 276, No. 5, 1963, pp. 385-393.

8. Blanchard, K.E. and Schultz, A.B., "On the Shock Response of Inelastic Beams", Journal of the Engineering Mechanics Division, Proceedings of ASCE, Vol. 91, No. EM5, October, 1965.

9. Heidebrecht, A.C., Fleming, J.F. and Lee, S.L., "Dynamic Analysis of Inelastic Multi-Degree Systems", Journal of the Engineering Mechanics Division, Proceedings of ASCE, Vol. 89, No. EM6, December, 1963.

10. Lee, S.L., "The Conjugate Frame Method and its Application in the Elastic and Plastic Theories of Structures", Journal Franklin Institute, Vol 266, No. 3, September, 1958, p. 207.

11. Heidebrecht, A.C., "Analysis of Dynamic Response of Inelastic Structural Systems", Ph.D. Thesis, Northwestern University, Evanston, Illinois June, 1963.

12. Fleming, J.F. and Romualdi, J.P., "A General Procedure for Calculating Dynamic Response Due to Impulsive Loads", Journal Franklin Institute, Vol. 275, No. 2, February, 1963, p. 107.

13. Beedle, Lynn S., Plastic Design of Steel Frames, John Wiley and Sons, Inc., New York, 1964, p.40.